JOURNAL OF GEOPHYSICAL RESEARCH, VOL. 94, NO. B1, PAGES 603–623, JANUARY 10, 1989

A More Precise Chronology of Earthquakes Produced by the San Andreas Fault in Southern California

KERRY SIEH

Division of Geological and Planetary Sciences, California Institute of Technology, Pasadena

MINZE STUIVER

Department of Geological Sciences and Quaternary Research Center University of Washington, Seattle

DAVID BRILLINGER

Department of Statistics, University of California, Berkeley

Improved methods of radiocarbon analysis have enabled us to date more precisely the earthquake ruptures of the San Andreas fault that are recorded in the sediments at Pallett Creek. Previous dates of these events had 95% confidence errors of 50–100 calendar years. New error limits are less than 23 calendar years for all but two of the dated events. This greater precision is due to larger sample size, longer counting time, lower background noise levels, more precise conversion of radiocarbon ages to calendric dates, and better stratigraphic constraints and statistical techniques. The new date ranges, with one exception, fall within the broader ranges estimated previously, but our estimate of the average interval between the latest 10 episodes of faulting is now about 132 years. Variability about the mean interval is much greater than was suspected previously. Five of the nine intervals are shorter than a century; three of the remaining four intervals are about two to three centuries long. Despite the wide range of these intervals, a pattern in the occurrence of large earthquakes at Pallett Creek is apparent in the new data. The past 10 earthquakes occur in four clusters, each of which consists of two or three events. Earthquakes within the clusters are separated by periods of several decades, but the clusters are separated by dormant periods of two to three centuries. This pattern may reflect important mechanical aspects of the fault's behavior. If this pattern continues into the future, the current period of dormancy will probably be greater than two centuries. This would mean that the section of the fault represented by the Pallett Creek site is currently in the middle of one of its longer periods of repose between clusters, and sections of the fault farther to the southeast are much more likely to produce the next great earthquake in California. The greater precision of dates now available for large earthquakes recorded at the Pallett Creek site enables speculative correlation of events between paleoseismic sites along the southern half of the San Andreas fault. A history of great earthquakes with overlapping rupture zones along the Mojave section of the fault remains one of the more attractive possibilities.

INTRODUCTION

Paleoseismology, the recognition and characterization of past earthquakes from evidence in the geological record, has contributed fundamentally to understanding earthquakes [*National Academy of Sciences*, 1986]. It has done so by extending the known record of earthquakes into past centuries and millennia. This extension of the historic and instrumental record has revealed not only more about the size, location, and timing of past large earthquakes; it has also yielded clues about the length and regularity of earthquake cycles and the variability of rupture magnitude and extent from event to event along a particular fault.

Imprecise dating of prehistoric events is a major obstacle to further progress in paleoseismology. This is a particularly troublesome problem along faults such as the San Andreas, where the imprecision in dating of paleoearthquakes has been approximately equal to the time between large earthquakes. In such cases, the imprecision of radiocarbon dating has prohibited the correlation of fault ruptures between paleoseismic sites and the recognition of patterns in the timing of earthquakes.

Paper number 88JB03635.
0148-0227/88/88JB-03635$05.00

Recent advances in conventional radiocarbon analysis now enable significantly greater precision in dating prehistoric and preinstrumental large earthquakes. Systematic high-precision measurements, using large proportional counters with extremely low backgrounds, have been conducted at the Seattle Quaternary Isotope Laboratory since 1973 [*Stuiver et al.*, 1979]. These counters require fairly large samples (about 7 g of carbon at Seattle) and have extremely low backgrounds. Whereas typical counters and accelerator mass spectrometric (AMS) analyses produce errors of the order of 50–100 years, the high-precision counters produce radiocarbon dates with standard errors of 12–20 years.

A sensible place to begin a program of more precise radiocarbon dating of earthquakes is at Pallett Creek, a paleoseismic site astride the San Andreas fault 55 km northeast of Los Angeles. This site contains a record of 12 large earthquakes preserved in interbedded marsh and stream deposits [*Sieh*, 1978*a*, 1984]. Previous radiocarbon dating of peaty beds within the strata revealed that the 12 earthquakes occurred within the past 1800 years. The average interval of dormancy between these earthquakes was shown to be about 145 years, but the dates of individual quakes and the length of individual recurrence intervals were not well established because of large error estimates in the radiocarbon dates.

Several other paleoseismic sites along the San Andreas fault in southern California have also yielded useful information about prehistoric earthquake ruptures along the fault [*Williams and Sieh*, 1987; *Sieh*, 1986; *Weldon and Sieh*, 1985; *Rust*, 1983; *Davis*, 1983; *Sieh and Jahns*, 1984]. Nevertheless, the sediments at Pallett Creek contain the most complete record of paleoearthquakes along the fault, and more precise dating of these earthquakes is the most logical first step in any attempt to correlate large earthquakes along the fault or to identify temporal patterns of earthquake occurrence.

DATES OF THE EARTHQUAKES AT PALLETT CREEK

The occurrence of earthquakes during the past two millennia is revealed by faults, folds, and liquefaction features within the marsh and stream deposits at Pallett Creek [*Sieh*, 1978*a*, 1984]. These structures and sedimentary features show that earthquakes have occurred at 12 specific times. These earthquakes are represented by 12 stratigraphic horizons within the marsh and streambed deposits. These horizons are labeled A–Z on the right-hand side of the columnar section depicted in Figure 1.

We have redated the 10 most recent of these earthquake horizons by radiocarbon analysis of overlaying and underlaying beds. The newly dated strata range from mid-unit 26, with an approximate date of A.D. 650, to unit 88, which formed just prior to the earthquake of A.D. 1857.

In the course of this study, 32 peat samples from 20 distinct strata were collected and analyzed. Table 1 lists all of the samples, from youngest to oldest, describes the nature of the sampled material, and gives other pertinent information.

The use of peat for dating the earthquakes at Pallett Creek has minimized the problem of contamination that sometimes complicates the use of other materials, such as detrital wood and charcoal. The peats formed in situ, unlike wood and charcoal, which may be derived from the heartwood of old trees or shrubs and thus be decades to centuries older than the stratum in which the sampled material is deposited.

Table 2 lists the same samples as those given in Table 1 but with the results of the new radiocarbon analyses. In column 3 are the radiocarbon ages of the samples (in years before present) and their standard errors. Multiple samples were collected from several of the sedimentary units as a test of reproducibility. In every case, the 2σ error ranges of the independent samples overlapped, and so weighted averaging of the ages was justified. Averaged radiocarbon ages for strata from which more than one sample was collected are listed in column 4.

These precise radiocarbon age determinations can be converted into precise calendric dates and error bands because high-precision calibration curves relating radiocarbon age to calendric date are now available. Recent progress in this field is given in the calibration issue of *Radiocarbon* [*Stuiver and Kra*, 1986]. The age conversions in this paper have been made using the bidecadal calibration curve of *Stuiver and Becker* [1986]. The microcomputer program that we used to transform the radiocarbon ages into calendric dates [*Stuiver and Reimer*, 1986], which includes the likelihood analysis explained in the appendix, is obtainable from the Quaternary Isotope Laboratory of the University of Washington on a DS/DD floppy diskette.

The calendric date ranges calculated from the calibration program are given in column 5 of Table 2. These are expressed as A.D. date ranges that span the 95% confidence interval.

Many of the units have ^{14}C age ranges that correspond to two or more calendric date ranges. Note, as an example, that the radiocarbon age of upper unit 68, 343.2 ± 11.7 years B.P. corresponds to two calendric date ranges, A.D. 1479–1523 and A.D. 1565–1631. This results from fluctuations in the $^{14}C/^{12}C$ ratio in the atmosphere during the past several millennia [*Stuiver and Kra*, 1986]. Figure 2 illustrates these irregularities in a graph of radiocarbon age versus calendric date.

The calendric date ranges were derived from the likelihood plots shown in Figure 3. These plots display in a convenient form the age information from a single sample or a combination of samples. The function plotted in each graph represents the relative likelihood of the date of the sample. The date ranges above the dashed horizontal lines indicate the 95% confidence interval for the actual date of the stratum. For a more detailed description of the likelihood plots and their creation, please refer to the appendix.

Figure 4 depicts the new radiocarbon ages for the 20 beds in order of their stratigraphic position. The reliability of the analyses is confirmed by the observation that only one of the 20 beds, unit 35, has a date that contradicts its stratigraphic position. The anomalously old date for unit 35 is probably due to the fact that this unit contains an abundance of charcoal and wood fragments (Table 1). This wood may well have been a century old at the time of its incorporation into the unit. This is the only peat sample in which we recognized, at the time of collection, wood and charcoal fragments; we collected and analyzed the sample, knowing that the sample age might well be older than the age of the stratum.

We are pleased that the new radiocarbon analyses do not, for the most part, contradict the previous age estimates by *Sieh* [1984]. Rather, they improve the precision of the earlier estimates.

What follows now is a discussion of the date of each of the past 10 earthquakes. We begin with a consideration of the sample that constrains the date of the youngest earthquake and end with an analysis of the three samples that constrain the date of the oldest earthquake. The data presented in Figures 1 and 3 and Table 2 are referred to throughout this discussion. You may wish to refer to these figures and this table to verify the stratigraphic and geochronologic assertions in the text that follows.

Event Z

Event Z is the latest event to rupture the sediments at Pallett Creek. *Sieh* [1978*a*, p. 3925; 1984, pp. 7646–7647] described evidence at the site for this event and concluded, on the basis of historical evidence, that this must be the fault rupture associated with the great Fort Tejon earthquake of 1857.

To test the reliability of our peat dates, we dated thin, peaty uppermost unit 88, which was at the ground surface in 1857, at the time of event Z. We were pleased to find that the calendric date ranges of this bed (A.D. 1691–1733 and A.D. 1814–1923 (Figure 3)) are, in fact, consistent with deposition in 1857.

Statistically, neither date range can be favored over the other. So, if we did not already know from the historical record that event Z is the earthquake of 1857, we would conclude that event Z occurred within either the interval A.D. 1712 (1691–1733) or the interval A.D. 1869 (1814–1923). This bolsters our confidence that no systematic errors exist in our

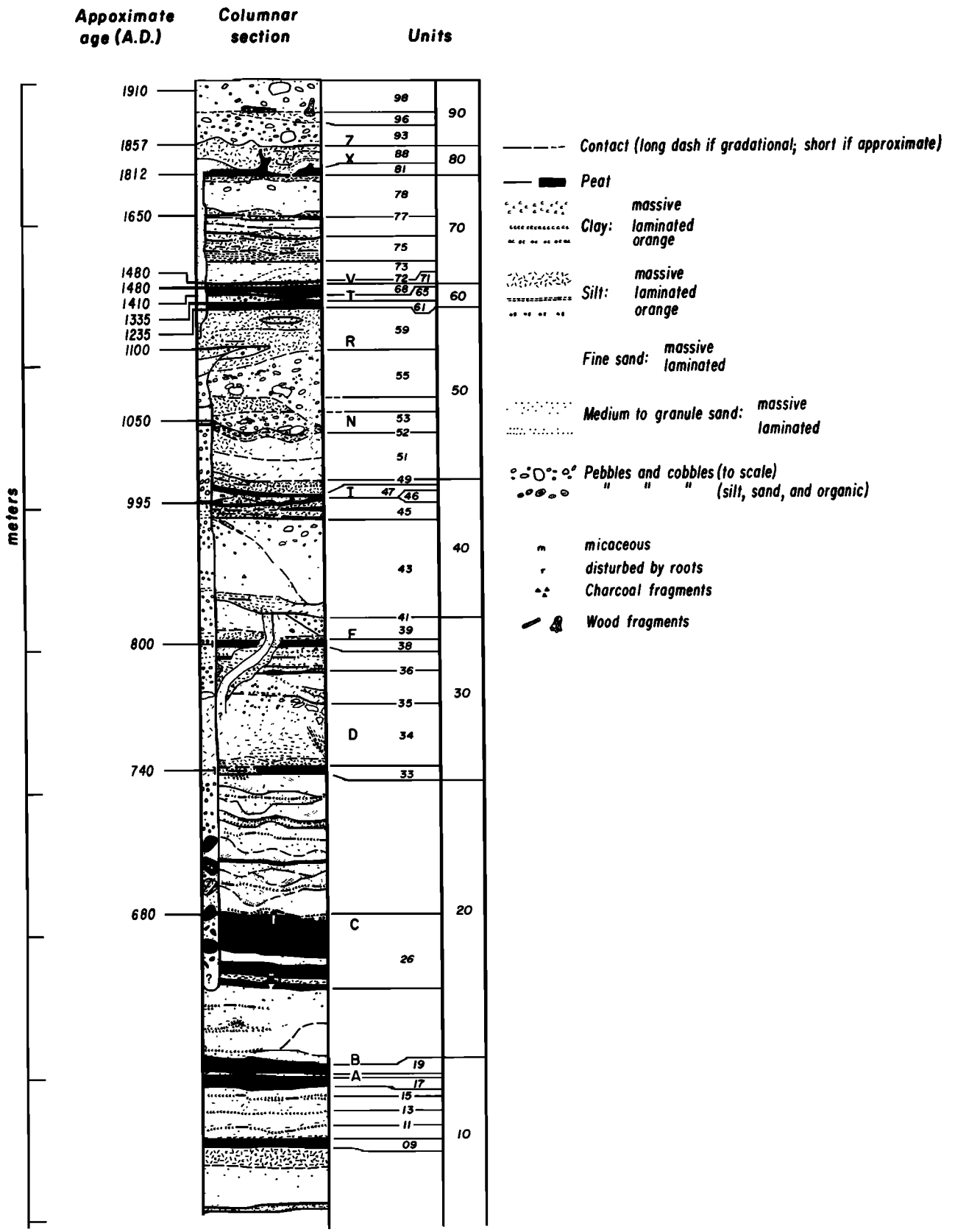

Fig. 1. The peats, silts, sands, and gravels at the Pallett Creek site were deposited during the past two millennia. The dates of deposition of several of the peaty beds are written to the left of the section. The locations of the 12 earthquake horizons are indicated by capital letters on the right, as are the numerical names of the beds mentioned in this paper.

TABLE 1. Radiocarbon Sample Descriptions

Sample*			
Lab (QL)	Field (PC)†	Unit Sampled	Sample Description
1990	86-(-114)-88-1	uppermost 88	Dry, flattened, long black fibers about 3 mm wide, collected from a discontinuous peat at top of unit 88. Sample comes from a loose fibrous mat of vertically and horizontally oriented fibers, which may represent a clot of grass growing in the marsh when this horizon was the ground surface. At the sample locality this bed clearly was warped vertically at the fault during event Z.
1980	85-137-u81	uppermost 81	Black peaty upper 1 cm of unit 81 beneath sandblow just south of event X and Z fault plane. Rootlets contaminating sample were removed by P. Haase prior to submission for analysis.
1981	85-81(N)	uppermost 81	Notes lost, but K. Sieh believes the sample was of the upper 1 cm of unit 81 about 25 m downstream from the main fault plane in the southeasternmost gorge wall at the site.
1991	86-81m	middle 81	Dry, lowest peaty part of unit 81, collected 28 m from exposure of main fault exposed in bulldozer cut at southeast end of terrace and 13 m from exposure 7 of *Sieh* [1978*a*]. Sample contains a few percent black detrital charcoal and a percent or so of white root hairs. Unit 81 here is 6.2 inches thick; lowest 3.0 inches is a light gray silt; next 0.7 inch is a brown/black fibrous peat; next 1.3 inches is a peaty gray silt; upper 1.2 inches is a black/brown fibrous peat.
1992	86-75	75	Dry, fibrous brown peat immediately below unit 78 sand, 26 m from exposure of main fault exposed in bulldozer cut at southeast end of terrace and 13 m from exposure 7 of *Sieh* [1978*a*]. White root hairs constitute <1% of sample.
1958	85-72	72	Black peat on southwest, gorge-facing wall 5–7 m southeast of southeast boundary of excavations in Figure 1 of *Sieh* [1984]. Vertical, paper-thin rootlets or stems projecting into the unit from a peat about 25 cm above unit 72 constitute <3% of the sample.
1994	86-72A	72	Thin, dry peat in exposure 138, about 1 to 2 m southwest of event X and Z main fault plane. Two dozen 1-mg root hairs removed from this sample.
1993	86-72	72	Thin, dry peat at south end of exposure 138, immediately north of sample PC85-72 locality. No contamination by younger rootlets is apparent.
1956	85-68	uppermost 68	Upper 1 cm of black peaty unit 68, on southwest, gorge-facing wall 5–7 m southeast of southeast boundary of excavations in Figure 1 of *Sieh* [1984]. Vertical, paper-thin rootlets or stems projecting into the unit from a peat about 25 cm above unit 72 constitute <3% of the sample.
1957	85-(-112)-68	uppermost 68	Black, peaty upper 1 cm of unit 68, 2 to 3 m southwest of the event Z fault plane in excavation -112. Unit 68 here consists of two light colored silty beds interbedded with peat.
1995	86-168	lowest 68	Lowest ~1.5 cm of dry, peaty unit 68, collected about 1–2 m southwest of event X and Z main fault plane. Sample contains a few percent pebbles from underlying unit 65 and a few percent black, charred(?) wood.
1954	85-61 (upper)	uppermost 61	Black, peaty upper 1–1½ cm of unit 61, about 25 m downstream from main fault plane in southeasternmost gorge wall. Unit 61 here is split into about four or five distinct peat layers, the youngest of which is about 2–3 cm thick.
1979	85-105.6-u61	uppermost 61	Black, uppermost two peat layers, which vary from 1 to 3 cm thick. Sampled from three localities about 2½ m apart in exposure -105.6. Unit 61 is about 12 cm thick here and consists of interbedded organic and inorganic beds. Clearly cut by event T sandblow a few meters to the southwest.
1953	85-61S	uppermost 61	Black, peaty upper 5 mm of massive 20- to 30-mm-thick unit 61, collected on both sides of minor fault shown in Figure 14 of *Sieh* [1978*a*], 9–12 m northeast of the main fault plane.
1955	85-61 (lower)	lowest 61	Black, 1-cm-thick peat 15 cm below the top of unit 61 and immediately beneath a coarse sand, about 25 m downstream from main fault plane in southeasternmost gorge wall. Bed sampled is above lowest bed in unit 61, which is 0–5 mm thick and discontinuous.
1978	85-105.6-L61	lowest 61	Thin, lowest, black, peaty bed of unit 61 blankets the southern shallow-dipping bank of deep channel cut into unit 50 prior to deposition of unit 61. Rootlet contamination ≪1%. No detrital charcoal apparent.
1977c	85-139-59c	59 fissure	Black peat about 20 cm thick on northwest wall of event R fissure. Collected from exposures about 20–50 cm southeast of exposure 138.5. Lower portions of peat-filled fissure probably removed by event T faulting, so this sample is probably the same age as sample 59a.
1977a	85-139-59a	59 fissure	Black peat 7–14 cm from base of event R fissure, collected in exposures 0–21 cm southeast from exposure 138.5.
1977b	85-139-59b	59 fissure	Black peat 0–7 cm from base of event R fissure, collected in exposures 0–21 cm southeast from exposure 138.5.
1976	85-206-47	47	Laminated 3 ± 0.2 thick peaty unit 47, collected from between the two major faults in exposure 206. Contamination by small rootlets is noticeable.
1952	85-47	47	Black peat quite free of rootlet contamination, 1–4 m north of main fault plane at bulldozer cut on southeast edge of site, about 4 m south of the fault shown in Figure 14 of *Sieh* [1978*a*].
1951	85-45	uppermost 45	~1-cm-thick black peat at top of unit 45; quite free of rootlet contamination, 1–4 m north of main fault plane at bulldozer cut on southeast edge of site, about 4 m south of the fault shown in Figure 14 of *Sieh* [1978*a*].

1975	85-206-43	43	Cylindrical twig about 1 cm in diameter and about 20 cm long with three or four annual rings visible and bark present locally. One end rounded, probably during transport. In silty, charcoal-rich and small-wood-fragment-rich unit separating the two gravelly sands that constitute unit 43. Collected about 1 m southwest of event X and event Z fault plane in exposure 206.
1974	85-206-41	41	Black peat of unit 41, 4–8 mm thick and immediately atop unit 39 gravel. No apparent contamination by rootlets.
1973	85-206-u38	uppermost 38	Clean (rootless) black peat from uppermost 8–15 mm of unit 38, separated at this locality from the underlying remainder of unit 38 by a thin, very coarse sand. Collected from between event T and event F fault planes in exposure 206.
1950	85-38	uppermost 38	Dark, upper 8 mm of unit 38, 2–3 m south of fault shown in Figure 14 of *Sieh* [1978*a*].
1972	85-206-35	35	Very silty gray to black peaty unit 35. Unit 35 at this locality is associated with wood and charcoal fragments, but only one ~6-mm-diameter twig was intentionally included in sample. Collected from four places on both sides of, and within about 2 m of, the event F fault plane in cut 206.
1971	85-206-u33	upper 33	The uppermost 3-mm-thick black peat of unit 33, 24–32 mm below the top of unit 33 at this locality, immediately north of the event F fault in cut 206.
1970	85-206-m33	middle 33	A 10-mm-thick black peat, the top of which is 42–48 mm below the base of the peat sampled as PC85-206-u33. Collected immediately north of the event F fault in cut 206.
1968	85-206-u26 upper ½	uppermost 26	Upper half of black, rhizomaceous 3-cm-thick peat that is the youngest bed of unit 26. Collected immediately north of the event F fault plane in cut 206.
1969	85-206-u26 lower ½	upper 26	Lower half of black, rhizomaceous 3-cm-thick peat that is the youngest bed of unit 26. Collected immediately north of the event F fault plane in cut 206. Event C occurred just before deposition of this bed.
1967	85-206-26	middle 26	Upper ½ of a black rhizomaceous peat, 13–14 cm below the top of unit 26. Collected immediately north of the event F fault plane in cut 206. Event C occurred just before deposition of this bed.

*Samples are listed in stratigraphic order, youngest first, oldest last.
†Field numbers in format xx-yyy-zzz and xx-zzz; "xx" indicates year of collection, "yyy" indicates exposure from which sample was collected, and "zzz" indicates stratum collected.

dates and that our radiocarbon dates allow accurate determination of the dates of the prehistoric earthquakes at the site.

Event X

Evidence for the occurrence of event X has been presented by *Sieh* [1978*a*, pp. 3923–3924; 1984, pp. 7646–7647]. This event rent the sediments at Pallett Creek when the top of unit 81 was the active surface of the marsh. No peat was deposited immediately after the event, so the best radiometric estimate of the date of the earthquake must be derived from determinations of the age of unit 81. For this reason, two samples of the uppermost 1 cm of unit 81 were collected and analyzed (QL-1981 and 1980, Tables 1 and 2).

A sample from the middle of unit 81 was also collected in order to allow determination of the rate at which unit 81 was deposited (QL-1991). This would have allowed extrapolation of the date of event X from the date of uppermost unit 81.

In actuality, the dates of uppermost and middle unit 81 are indistinguishable (165–183 ^{14}C years B.P., with standard errors of 9–16 years). So, by multiplying the individual likelihood functions, we merged the three ages in order to derive a date range for upper unit 81:176.5 $\pm$ 6.8 ^{14}C years B.P. Unfortunately, this radiocarbon age corresponds to three calendric date ranges: A.D. 1669–1679, 1741–1801, and 1939–1955. The latter range can, of course, be ruled out on historical grounds and by virtue of the fact that unit 81 must be older than uppermost unit 88, which, according to the date of sample QL-1990, was deposited before 1923. The remaining two ranges have comparable likelihoods of containing the actual date of formation of uppermost unit 81 (Figure 3).

To derive the date ranges for event X, we must now estimate the amount of time that passed between deposition of the samples of uppermost 81 and the occurrence of the earthquake. Unfortunately, the rate of accumulation of unit 81 can not be calculated from the available data. However, the rates of accumulation for two similar peats, units 61 and 68, can be calculated from the dates now available. We will show later in this paper that these peaty beds accumulated at rates between 0.2 and 2.1 mm/yr. The samples of uppermost 81 that we collected included the upper 10 mm of the bed. If we assume that our date ranges represent the date of deposition of the central plane of the sample, about 5 mm of peat accumulated before the occurrence of event X. Thus we conclude that 14 $\pm$ 12 years elapsed between the time of deposition of the samples and the time of the earthquake.

This amount of time must be added to the date ranges of the samples to estimate the date ranges for the earthquake. The date ranges thus calculated for event X are A.D. 1688 (1675–1701) and A.D. 1785 (1753–1817).

We prefer to reject the older of these two ranges because of its proximity to the date range of an underlying bed, unit 75. The date range of unit 75 is A.D. 1648 (1639–1657). About 100 mm of peat and silt lay between unit 75 and the horizon of event X [*Sieh*, 1978*a*]. Deposition rates would have to be very high (2 mm/yr) for unit 75 to have been deposited A.D. 1648 (1639–1657) and event X to have occurred no more than a few decades later. About 150 mm of silt and peat lie between units 72 and 75 [*Sieh*, 1978*a*]. From the radiocarbon analyses of these two beds we know that this sediment accumulated in 175 $\pm$ 18 years at an average rate of deposition of 0.9 $\pm$ 0.1 mm/yr. If the 100 mm of peat and silt between unit 75 and the event X horizon accumulated at this rate, event X would have

TABLE 2. Radiocarbon Analyses

Sample*		^{14}C Age, years B.P.	Averaged ^{14}C Age,‡ years B.P.	Calendar Age,§ A.D.
Lab (QL)	Field (PC)†			
1990	86-(-114)-88-1	93.0 ± 16.2		1814–1923 1691–1733
1980	85-137-u81	171.5 ± 12.8		
1981	85-81(N)	183.0 ± 9.3	176.5 ± 6.8	1939–1955 1741–1801 1669–1679
1991	86-81m	165.0 ± 16.1		
1992	86-75	260.0 ± 16.3		1639–1657
1958	85-72	394.7 ± 12.2		
1994	86-72A	374.0 ± 15.2	382.0 ± 8.1	1457–1489
1993	86-72	370.0 ± 15.4		
1956	85-68	344.5 ± 16.6	343.2 ± 11.7	1565–1631 1479–1523
1957	85-(-112)-68	342.0 ± 16.5		
1995	86-168	542.0 ± 15.0		1397–1419 1329–1331
1954	85-61 (upper)	572.4 ± 12.8	579.3 ± 8.5	1387–1401 1317–1351
1979	85-105.6-u61	571.0 ± 15.2		
1953	85-61S	601.4 ± 16.9		
1978	85-105.6-L61	814.0 ± 15.4		
1955	85-61 (lower)	816.3 ± 14.6	815.1 ± 10.6	1215–1250
1977c	85-139-59c	854.0 ± 15.5	859.8 ± 11.1	1165–1220
1977a	85-139-59a	866.0 ± 16.0		
1977b	85-139-59b	906.0 ± 13.6		1041–1167
1976	85-206-47	1005.0 ± 16.2	1032.5 ± 11.3	985–1017
1952	85-47	1058.3 ± 15.7		
1951	85-45	1076.1 ± 17.1		952–999 899–911
1975	85-206-43	1211.0 ± 57.6		
1974	85-206-41	1227.0 ± 15.8		
1950	85-38	1215.0 ± 16.7	1221.6 ± 9.2	775–819
1973	85-206-u38	1223.0 ± 15.8		
1972	85-206-35	1443.0 ± 17.0		595–645
1971	85-206-u33	1291.0 ± 15.8	1274.4 ± 11.0	679–773
1970	85-206-m33	1259.0 ± 15.7		
1968	85-206-u26 upper ½	1270.0 ± 15.8		679–779
1969	85-206-u26 lower ½	1323.0 ± 16.2		661–687
1967	85-206-26	1401.0 ± 14.1		627–657
A-2154	415b peat		1648 ± 38.4	477–529 323–464 259–293
A-2151	415b cell			
USGS-899	414d	1832 ± 56		277–336 60–266
USGS-898	414j	1894 ± 64		B.C. 46–A.D. 252

*Samples are listed in stratigraphic order, youngest first, oldest last.

†Field numbers in format xx-yyy-zzz and xx-zzz; "xx" indicates year of collection, "yyy" indicates exposure from which sample was collected, and "zzz" indicates stratum collected.

‡These standard errors include all variability encountered in the laboratory procedure. A substantial portion of the error is related to the Poisson error in the observed number of decaying ^{14}C atoms (standard deviation equal to the square root in the number of counts). Many laboratories report only this error. However, estimation of the true error in the measurement of the age of the sample must include other factors. From a comparison of measurements on duplicate samples, we find that the Seattle ages have standard errors compatible with 1.2–1.6 times the error based on counting statistics alone (for example, see *Stuiver* [1982]). All age errors given in this paper are based on a liberal 1.6 error multiplier. The quoted age errors thus account for the entire variance in the measuring procedure.

§Ranges include values within 95% confidence limits.

occurred 113 ± 13 years after deposition of unit 75, that is, A.D. 1761 (1745–1777). This range is within the younger of the two ranges given for event X. For these reasons, we prefer the younger of the two statistically plausible date ranges, A.D. 1785 (1753–1817). We caution, however, that the older date range, A.D. 1674 (1669–1679), can not be unequivocally excluded on the basis of this argument. Information discussed in the following paragraph lends additional support to our belief that event X occurred during the period A.D. 1785 (1753–1817).

Previous radiocarbon analyses yielded a range of A.D. 1750 (1670–1830) for event X. *Sieh* [1984, Table 2] concluded that the portion of this range that postdated 1768 could be excluded because of a lack of historical large earthquakes since the advent of Europeans in southern California in 1769. Recently, however, *Jacoby et al.* [1987, 1988] found clear dendrochronologic evidence of fault rupture 13–25 km southeast of Pallett Creek in late 1812 or early 1813. This led them to reevaluate the felt reports for the "San Juan Capistrano" earthquake of December 8, 1812, and to conclude that this earthquake was probably produced by rupture of the San Andreas fault along a reach at least several tens of kilometers in length and including the Pallett Creek site. Event X is the only event at Pallett Creek with a date range that is compatible with a date of December 8, 1812. We suspect, therefore, that event X is the large historical earthquake that occurred on that date.

Event V

Evidence for event V has been presented by *Sieh* [1978*a*, p. 3922; 1984, pp. 7647–7649]. This large earthquake occurred between deposition of upper unit 68 and unit 72. At the time of the earthquake the upper surface of unit 68 was the active surface of the Pallett Creek marsh. Furthermore, stratigraphic evidence strongly indicates that unit 72 was deposited within a few years of the earthquake. We suspected that the radiocarbon analyses of these two beds would yield indistinguishable date ranges and provide a very tight constraint on the date of intervening event V.

The five new radiocarbon analyses of units 68 and 72 do, in fact, constrain the date of event V very tightly. The date ranges of upper unit 68 are A.D. 1479–1523 and A.D. 1565–1631. The date range of unit 72 is A.D. 1457–1489. Unit 72 is stratigraphically above unit 68, so it must be younger. This clearly rules out the A.D. 1565–1631 range for upper unit 68.

The remaining date range for upper unit 68 overlaps the date range of unit 72. Hence we may legitimately merge the radiocarbon ages of the two units to derive the radiocarbon age of event V. That age, 369.5 ± 6.7 ^{14}C years B.P., corresponds to a calendric date range of A.D. 1480 (1465–1495).

A very small peak in the likelihood function for event V also exists at about A.D. 1610 (Figure 3). The likelihood that the earthquake occurred at that time is about one thirtieth the likelihood that it occurred in about A.D. 1480. For this reason, we are quite confident that event V occurred in about A.D. 1480.

Event T

Evidence for event T is documented in previous papers [*Sieh*, 1978*a*, pp. 3921–3922; 1984, pp. 7649–7650]. This earthquake occurred when the top of unit 61 was the surface of the marsh. Therefore the date ranges of upper unit 61 should closely approximate the date of the earthquake. Our estimate

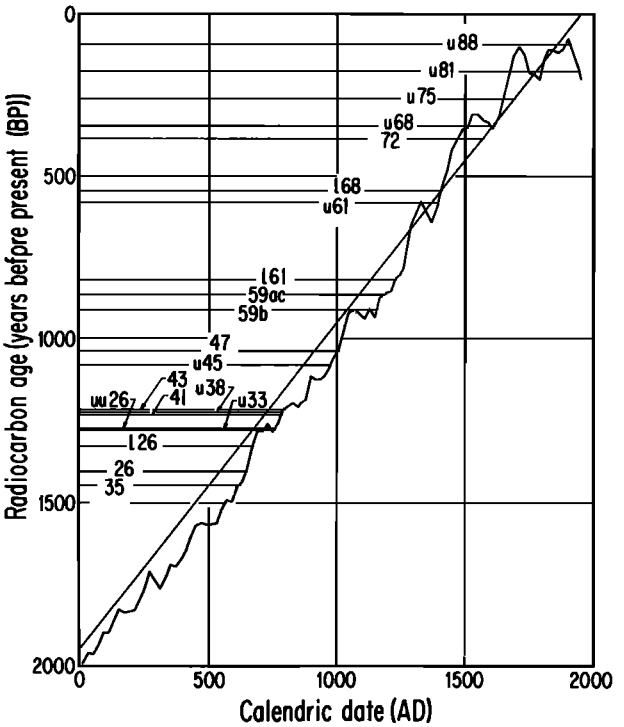

Fig. 2. Fluctuations in the atmospheric ratio of ^{14}C to ^{12}C has resulted in an irregular relationship between analytically determined radiocarbon age (years before present, B.P.) and actual calendric date (A.D.). Radiocarbon analyses performed for this study are shown by the horizontal lines. Note that many of these analyses yield multiple choices for the calendric date of the sample. Diagonal line is locus of points where radiocarbon age is equal to calendric date (for example, 0 B.P. = A.D. 1950) [from *Stuiver and Becker*, 1986].

of the date of event T is based upon the date ranges of upper unit 61, with a minor correction that allows for sedimentation that occurred between the central plane of the samples and the earthquake horizon.

Three separate samples of upper unit 61 yielded similar radiocarbon ages, which when merged give calendric date ranges of A.D. 1317–1351 and A.D. 1387–1401. Because the stratigraphic centers of the dated samples are several millimeters below the event T horizon, the date ranges for the earthquake should be a few years younger than these ranges.

A sedimentation rate for unit 61 can be estimated using the date ranges of upper and lower unit 61, according to the equation, $R = T/t$, where R is the average sedimentation rate, T is the thickness of intervening sediment, and t is the time between deposition of the two samples. In the case of unit 61, samples from the uppermost and lowest parts yield dates that are 101 ± 25 years apart (Table 2). (For reasons that are explained later in the paper, the younger range for uppermost unit 61 (A.D. 1387–1401) can be rejected.) The stratigraphic distance between the central planes of these samples is about 220 mm, at locations where the unit is uniform black peat. From this thickness and time difference we derive a sedimentation rate of 0.22 ± 0.06 mm/yr. Dividing this rate into the half thickness of the samples (2.5 mm) indicates that the earthquake is 12 ± 3 years younger than the date ranges of upper unit 61. The date thus derived for event T is A.D. 1346 (1329–1363) or A.D. 1406 (1398–1414).

The likelihood plot for upper unit 61 in Figure 3 shows

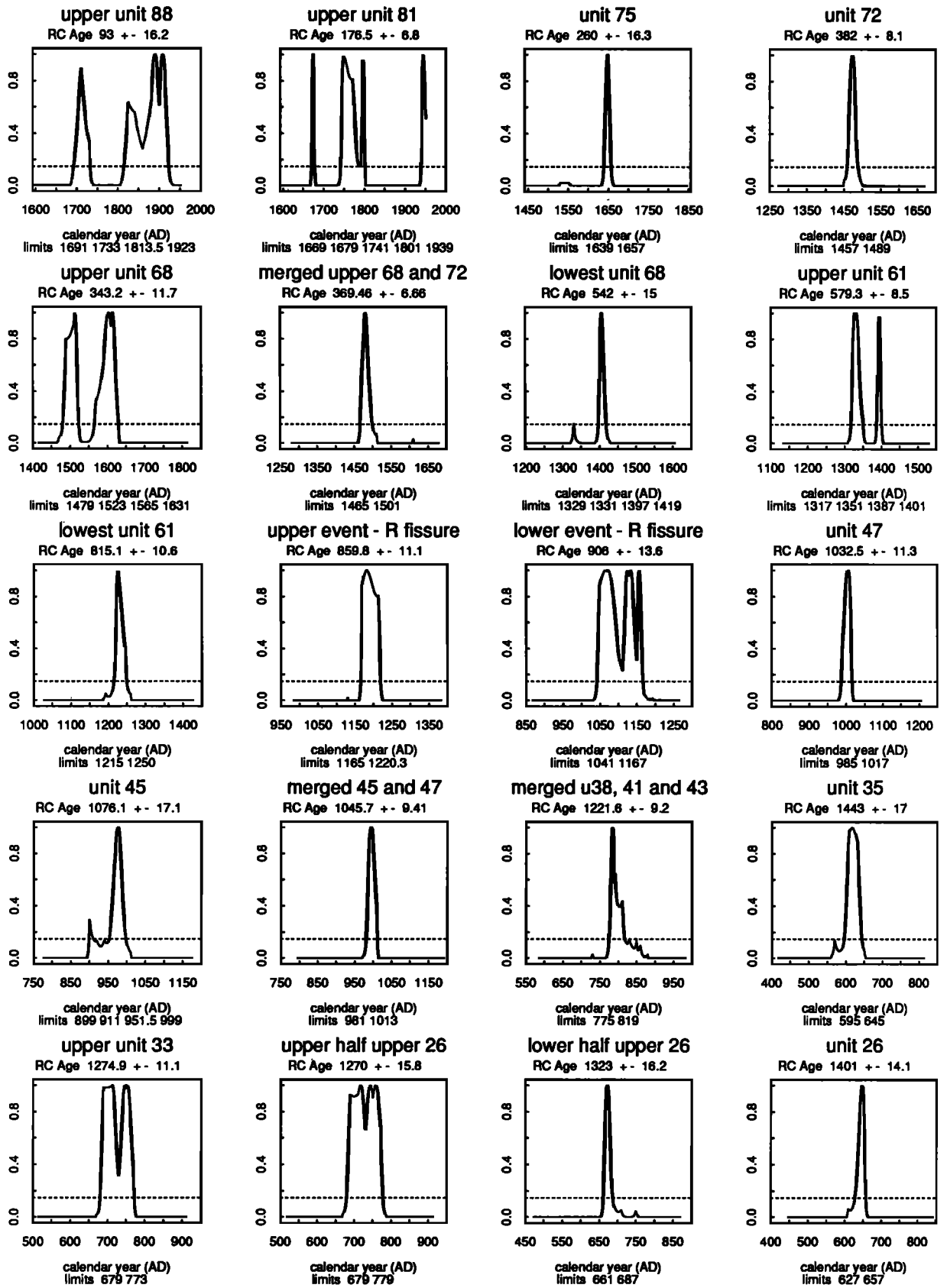

Fig. 3. Likelihood function plots for various radiocarbon ages. The dashed horizontal line defines the 95% confidence limits.

more area under the peak of the older date. A case in favor of the earlier range can also be made on the basis of the stratigraphic argument presented below.

Lowest unit 68 is the first peat to have been deposited subsequent to event T, so its date ranges of A.D. 1397–1419 and A.D. 1329–1331 are the best younger bound for event T. Figure 3 shows that the older of these two ranges is statistically quite unlikely; the older range can also be ruled out on the basis of the following stratigraphic argument. Extensive bioturbation, probably representing at least a few decades, occurred between event T and the initiation of deposition of unit 68 [*Sieh*, 1978*a*, p. 3933 and plate; 1984, pp. 7658 and 7669]. Therefore a date of A.D. 1329–1331 for lowest unit 68 would suggest a date for event T in the very early 1300s or late 1200s; this is an unacceptable date, because it is several decades older than the oldest plausible dates calculated for event T two paragraphs above.

This leaves only the date range of A.D. 1397–1419 for deposition of lower unit 68. If one allows at least 25 years for bioturbation between event T and the deposition of lower unit 68, the occurrence of event T after A.D. 1394 must be deemed quite unlikely. This seems to rule out the A.D. 1406 (1398–1414) date range for the earthquake calculated from the date ranges of upper unit 61 and leaves A.D. 1346 (1329–1363) as the best estimate for the date of event T.

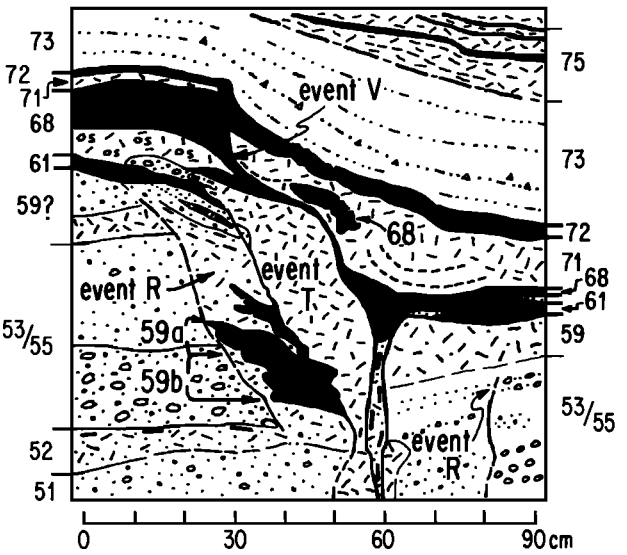

Fig. 5. This map of a vertical exposure displays a fissure that first formed during event R and was reopened during events T and V. Peat deposited in the fissure soon after event R provides the best limiting date for that event. This exposure is a few centimeters southeast of the southeasternmost excavation mapped by *Sieh* [1984]. Black beds are peats; stipples represent sand; short lined pattern indicates silt.

Event R

Evidence for event R was evaluated by *Sieh* [1978*a*, p. 3921; 1984, pp. 7650–7653]. Unlike every other seismic horizon in the sediments at Pallett Creek, no blanket of peat occurs either immediately beneath or immediately above the event R horizon. This presents a problem in dating the earthquake precisely. The stratigraphically nearest dated peat beds are subjacent unit 47 (A.D. 985–1017) and superjacent lower unit 61 (A.D. 1215–1250). These provide only very loose constraints on the date of the earthquake: it must have occurred within 130 years of A.D. 1120.

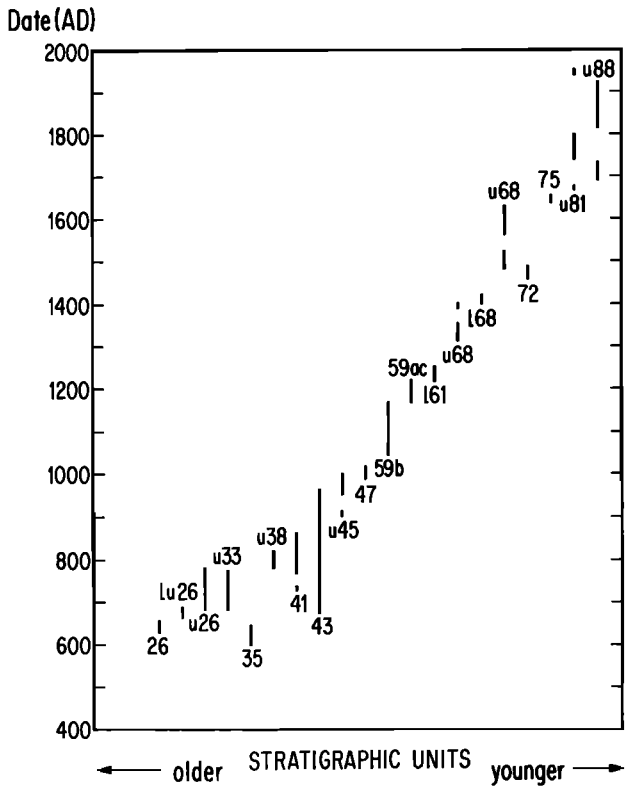

Fig. 4. This plot of calendric date versus stratigraphic position shows the internal consistency of the radiocarbon analyses performed for this study.

Fortunately, a fissure that formed during event R and was later filled with peat provides a narrower constraint on the date of the earthquake. The fissure was not described in previous papers, so we include Figure 5, a sketch of the vertical exposure from which two of the three peat samples were collected.

The most recent disturbance recorded in Figure 5 is associated with event V. At that time, unit 68 was disrupted along the fault plane labeled "event V." A previous event is represented by a silt-filled fissure to the left of the "event V" fault. That the fissure was produced during event T is indicated by its stratigraphic position between units 61 and 68. The right (southwestern) half of the material that filled this fissure was removed from the plane of this exposure by right-lateral slip along the "event V" fault.

To the left of the "event T" fissure is an older fissure filled with peat, silty sand, and sandy silt. This fissure cuts the gravels of unit 53/55 and is overlain by unit 61. This demonstrates that the fissure is in the stratigraphic position of event R, and so the fissure is ascribed to that event. (The previous event, N, occurred prior to deposition of unit 53 [*Sieh*, 1978*a*, pp. 3920–3921; 1984, p. 7653], and the subsequent event, T, occurred after deposition of unit 61 [*Sieh*, 1978*a*, pp. 3921–3922; 1984, pp. 7649–7650].)

In the exposure illustrated by Figure 5, peat fills the lowest 14 cm of the fissure. The upper half of the peat was collected as QL-1977a and QL-1977c and has a calendric range of A.D. 1165–1220. The lower half of the peat, which was collected as QL-1977b, has a calendric range of A.D. 1041–1167.

The date of QL-1977b should closely approximate the date of the earthquake. The loosely consolidated materials in the steep wall of the fissure would not likely have remained uneroded if the fissure had remained open more than a couple of decades. One would expect partial infilling of such a fissure within the first few months and years of its creation, and nearly complete filling could be expected within a few decades. So, we conclude that event R does not predate A.D. 1041–1167 by more than a decade or two. Hence event R probably occurred between A.D. 1021 and 1167.

The older part of this range can be trimmed on stratigraphic grounds. The section of gravelly sand between unit 47 and the event R horizon is about a meter thick. Deposition of this unit probably took place over a period of at least 50 years because unit 90, a much thinner section of similar gravelly sands, was deposited between A.D. 1857 and about 1910 [*Sieh*, 1978*a*]. Also, unit 52, within this coarse clastic section, locally shows evidence of incipient establishment of vegetative cover [*Sieh*, 1978*a*], indicating the passage of time. So, event R probably occurred at least 50 years after deposition of unit 47, that is, after about A.D. 1035.

From the arguments given above, the best estimate for the date range of event R is A.D. 1100 (1035–1165).

Event N

The evidence for event N was presented by *Sieh* [1978*a*, pp. 3920–3921; 1984, p. 7653]. *Sieh* [1978*a*] documented that event N occurred soon after deposition of unit 52 and just prior to deposition of thick, gravelly unit 53. Unfortunately, peat in unit 52 is quite rare, and none was exposed in the excavations made in the course of the current study.

The date of event N must therefore be interpolated between the dates of event I and event R. We have calculated a date range of A.D. 1100 (1035–1165) for event R. In the next section we will calculate a date range for event I of A.D. 997 (981–1013). Event N most likely occurred at least a few decades before the occurrence of event R because the deposition of gravelly alluvial unit 53 occurred between these two earthquakes. Event N also probably occurred at least a few decades after the occurrence of event I because several tens of centimeters of sandy, silty sediment were deposited between the two events and because unit 52 locally displays evidence of incipient soil formation. These observations are not readily quantifiable, but we judge that they allow us to narrow the limits for the date of event N by a few decades on each end.

In our judgment, the beds between the horizons of event N and event R represent about the same amount of time as do the beds between the horizons of event N and event I. Our best estimate for the date of event N is therefore the midpoint between events I and R: A.D. 1048. An alternate motivation for this estimate is that if the times between earthquakes are identically distributed random variables, then the midpoint is the expected location of the missing date. (Precisely, $E\{x|x + y\} = (x + y)/2$, with x, y referring to successive interval lengths.) We have estimated an error of 33 years for this date using the relationship that the variance of $(x + y)/2$ is $(\text{Var } x + \text{Var } y)/4$ for uncorrelated random variables x and y.

Event I

Evidence for event I has been described by *Sieh* [1978*a*, pp. 3919–3920; 1984, p. 7653]. The date of this earthquake is very tightly constrained by the dates of the immediately subjacent and superjacent units, 45 and 47. These two peaty beds are in physical contact except in those places at the site where sandblows erupted onto the surface of unit 45 during event I.

Unit 47 provides a young bounding range of A.D. 985–1017, and unit 45 provides an old bounding range of A.D. 899–911 or A.D. 952–999. The older of the two ranges for unit 45 can be excluded for two reasons: First, Figure 3 shows that the younger range is 3 times more likely than the older range to contain the date of the earthquake. Second, it is quite clear stratigraphically that deposition of unit 47 followed deposition of unit 45 very closely. Hence deposition of unit 45 occurred within the range A.D. 952–999.

Because the stratigraphic relationship of units 45 and 47 is so intimate, one can conclude that deposition of the two beds almost certainly occurred within the same decade. Hence it is justifiable to merge the radiocarbon ages of the two beds to determine the radiocarbon age of event I. The age of event I, determined in this manner, is 1045.7 ± 9.4 ^{14}C years B.P. This corresponds to a calendric date range of A.D. 997 (981–1013).

Event F

Event F is one of the more fully documented and understood events at Pallett Creek [*Sieh*, 1978*a*, pp. 3911–3919; 1984, pp. 7654–7655]. This earthquake occurred when the top of peaty unit 38 was the surface of the marsh. Overlaying unit 38 is unit 39, which consists of sand that was ejected from sandblows during event F and fluvial sand that filled many sandblow craters still open after the earthquake. In many exposures the sandblow deposits display evidence of fluvial erosion that occurred prior to deposition of the fluvial sand. Overlaying the sands of unit 39 is a thin black to gray peaty bed, unit 41. Unit 41 is, in turn, overlain by unit 43, which consists of two sandy fluvial beds separated by a septum that is locally rich in small wood and charcoal fragments.

The dates of deposition of uppermost unit 38 and unit 41 were expected to bracket the date of event F, with the date of unit 38 closely approximating the date of the earthquake and the date of unit 41 being several decades younger than the earthquake. In fact, we were pleasantly surprised to find that the dates of uppermost unit 38, unit 41, and unit 43 are statistically indistinguishable. This led us to merge the four radiocarbon ages of these three strata to determine a date range for event F of A.D. 775–819, that is, A.D. 797 (775–819).

Event D

Event D occurred during deposition of the lower, finer-grained portions of unit 34 [*Sieh*, 1978*a*, p. 3919; 1984, p. 7655]. Unit 33 is the last peaty bed deposited before event D, and unit 35 is the first peaty bed deposited after the earthquake. We collected samples from both unit 33 and unit 35 in order to place young and old bounds on the date of event D. Stratigraphic evidence suggests that unit 35 formed quite some time after event D, so we expected that we would not be able to merge the date of unit 33 with that of unit 35 to derive the date of the intervenient event. Therefore we collected samples not just from one but from two horizons within unit 33 in order to determine a sedimentation rate for the unit. We anticipated that this would allow us to extrapolate the date of the earthquake from the date of upper unit 33.

Unfortunately, the dates of samples from unit 33 are too imprecise to yield a useful sedimentation rate or a precise older bound for the earthquake, and unit 35 provided an unreliable date.

We had anticipated the latter problem; in our field notes we

mentioned the presence of small wood and charcoal detritus that might lead to an anomalously old date for unit 35. The date determined for unit 35 is, in fact, about a century older than the dates determined for the next four samples collected from subjacent horizons. Because of this, we do not believe that the date determined for unit 35 represents the actual date of deposition of the stratum and, accordingly, have not used it to constrain the date of event D.

The best constraint on the date of event D is the date range of unit 33: A.D. 679–773. This range for unit 33 is an older bounding range for the earthquake, but the sampled stratum lies several centimeters below the earthquake horizon.

The best estimate of the date of event D can be calculated using the date range of event F, A.D. 797 (775–819), as a younger bounding range and the date range of event C, A.D. 671 (658–684), as an older bounding range.

About 250 mm of silt, clay, and peat were deposited during the interval between event C and event D, and a similar thickness of fines was deposited during the period between event D and event F. If the average rate of deposition for these sediments, above and below the horizon of event D, are equal, then events C and D must be separated by 63 ± 13 years, and events D and F must be similarly separated. This suggests a date range for event D of A.D. 734 (721–747).

Event C

Event C was recognized and documented by *Sieh* [1984, p. 7655]. Three new radiocarbon analyses of unit 26 constrain the date of this event to about A.D. 680. Unit 26 is the peaty, clayey unit that contains the earthquake horizon. Two samples were collected from the lower and upper halves of a 30-mm-thick black peat immediately overlaying the event C horizon. The third sample was collected from a black peat 105 mm below the earthquake horizon. The fact that the sample date ranges are in agreement with their stratigraphic ordering gives us confidence in our estimate of the date of event C.

The 15-mm-thick sample representing the upper half of the bed that blankets the earthquake horizon (QL-1968) yielded a date range of A.D. 679–779. The 15-mm-thick sample representing the lower half of the same bed (QL-1969) gives a narrower date range of A.D. 661–687. The date of event C is within or a few years prior to the range of this sample. Sample QL-1967, taken from a peat bed about 140 mm below the event C horizon yielded an older bounding range of A.D. 627–657.

Sedimentation rates calculated from the difference in age of sample QL-1969 and QL-1967 can now be used to refine our estimate of the date of event C. The time that elapsed between deposition of these two samples is 41 ± 30 years. The stratigraphic distance between the central planes of the samples is 113 mm. The sedimentation rate calculated from these values is $2.8\ +7.5/-1.2$ mm/yr. The central plane of sample QL-1969 is about 8 mm above the event C horizon, so the date of event C is 3 ± 2 years older than the date of the sample. Subtracting this from the date range of QL-1969 yields our best estimate for the date range of the earthquake: A.D. 671 (658–684).

Events B and A

Events B and A are represented by fault ruptures identified by *Sieh* [1984, pp. 7655–7658]. Samples of the peaty beds above and below the horizons of events A and B were not collected for this study because exposure of the excavation in which these events were recognized by *Sieh* [1984] would have required the removal of 5–8 m of fill, far more than our budget allowed.

Because the beds above and below the event A and event B horizons were not resampled, the only ^{14}C ages pertinent to estimating the dates of these events are those reported by *Sieh* [1984, Table 3]. We have recalculated the date ranges for those samples by the calibration and likelihood estimation techniques that we have used for all of the new samples. The new date ranges are therefore greater than those calculated for the *Sieh* [1984] paper because of the incorporation of the "lab error multiplier" discussed in footnote to the averaged ^{14}C age of Table 2.

Event A occurred after deposition of sample USGS-898 and before deposition of samples USGS-899, A-2154, and A-2151 [*Sieh*, 1984]. Thus the earthquake occurred after B.C. 46 to A.D. 252 and before A.D. 60–529. The spread in age ranges for the older and younger bounding strata are so great that a useful estimate of the date of event A cannot be made.

Event B is also impossible to date precisely from the old radiocarbon analyses. It occurred soon after deposition of USGS-899, A-2154, and A-2151, which yielded ages ranging from A.D. 60 to A.D. 529. About the only useful conclusion one can draw about the date of event B is that it probably preceded the occurrence of event C by at least a century and a half.

DISCUSSION OF PALLETT CREEK EARTHQUAKE DATES

Comparison of New Dates With Those Previously Reported

Table 3 tabulates and Figure 6 displays the new date estimates for the past 10 earthquakes recorded at Pallett Creek. Figure 7 provides a comparison of the new earthquake dates and those derived from radiocarbon analyses published earlier. It is encouraging that all but one of the new date estimates are enclosed within or overlap the broader date ranges of *Sieh* [1984]. And the one new date range that does lie outside of the previous estimates, that of event C, misses overlapping with the previous range by only about a decade.

This comparison with the previous date estimates demonstrates that the old date ranges, though much less precise, are consistent with the new date ranges. The dates are now so much more precise that deviations from the average interval can be confidently identified.

Possibility of Missing Events

Before we discuss the significance of the new dates and recurrence intervals, we must consider the possibility of missing events, that is, events that ruptured the Pallett Creek sediments but have gone unrecognized.

Sieh [1984, p. 7669] argued that the 12 earthquake horizons now recognized at Pallett Creek are the only horizons he exposed that are associated with liquefaction or faulting at the site. Based upon his arguments, the possibility of an unrecognized earthquake horizon seems remote.

However, the possibility that two large earthquakes might be represented by only one earthquake horizon is not so readily dismissed. The sediments at the site were not deposited continuously, so it is conceivable that two earthquakes occurred without an intervening episode of marsh or stream

TABLE 3. Estimated Dates of Occurrence for Earthquakes at Pallett Creek

Event	Date Range,* A.D.	Basis for Determination
Z	Jan. 9, 1857	The date ranges of upper unit 88, which directly underlays the earthquake horizon, are A.D. 1712 (1691–1733) and A.D. 1869 (1814–1924). These are consistent with the historical record of a great earthquake in southern California and fault rupture in the Pallett Creek area in 1857.
X	Dec. 8, 1812	The date ranges of upper unit 81, which directly underlays the earthquake horizon, are A.D. 1674 (1669–1679) and A.D. 1771 (1741–1801). An additional 14 ± 12 years elapsed between deposition of the sample and occurrence of the earthquake. The radiocarbon estimate of the event is therefore A.D. 1785 (1753–1817) or 1688 (1675–1701). The latter range is unlikely, on stratigraphic grounds. Dendrochronologic and historical data of *Jacoby et al.* [1987, 1988] support a date of December 8, 1812, for this earthquake.
V	1480 (1465–1495)	From stratigraphic evidence, unit 72 overlays the earthquake horizon and was deposited very soon after upper unit 68, which directly underlays the earthquake horizon. The date ranges of these two units are very similar and are merged to estimate the date of the earthquake.
T	1346 (1329–1363)	From stratigraphic evidence, event T occurred soon after the deposition of upper unit 61 and several decades before deposition of lowest unit 68. This date range for event T results from analysis of the date ranges of units 61 and 68, considering both stratigraphic and statistical details.
R	1100 (1035–1165)	The date of this earthquake is constrained by the date range of a peat sample from an event R fissure. It is also constrained by the date range of unit 47, below.
N	1048 (1015–1081)	Distant younger and older limits for event N are the date of event R and the date of event I, respectively. Stratigraphic relationships suggest event N occurred about midway between the occurrence of event N and event I.
I	997 (981–1013)	From stratigraphic evidence, unit 47, the stratum overlaying the earthquake horizon, was deposited very soon after upper unit 45, the stratum underlaying the earthquake horizon. The radiocarbon ages for these two beds overlap and have been merged to estimate the date of the earthquake.
F	797 (775–819)	The radiocarbon age of unit 38, which directly underlays the earthquake horizon, is statistically indistinguishable from the radiocarbon ages of units 41 and 43, which overlay the earthquake horizon. The ages of these units have been merged to yield the date of the earthquake.
D	734 (721–747)	The date range of upper unit 33 provides an older bound for the date of event D. The range chosen here, however, is based upon interpolation between the dates of events C and F, using calculated sedimentation rates.
C	671 (658–684)	The peat directly above the earthquake horizon provides the closest estimate of the date range of event C. A minor adjustment to the peat's date range is made in order to allow for sedimentation after the earthquake and before deposition of the peat sample.
B	before 529	A.D. 529 is the youngest bound for the horizon that immediately underlays the event B horizon.

*Numbers followed by numbers in parentheses indicate 95% confidence intervals and their midpoints.

sedimentation. If this has happened at the site, one earthquake horizon would represent more than one earthquake.

Some large historical earthquakes are known to have occurred only a few hours, days, or years after nearby events. In most cases (for example, the great Alaskan/Aleutian earthquakes of 1957–1965, the Turkish events of 1939–1944, and the Japanese earthquakes of 1944–1946) neighboring segments of large faults broke, with little or no overlap. So, the possibility of minor overlap of fault ruptures during very closely timed events seems remote, but it can not be ruled out. One can argue that the chance of any one paleoseismic site being in the short overlap zone of large earthquake ruptures is very small; nevertheless, the possibility that the Pallett Creek site is so situated cannot be dismissed at this time. Discrimination of two slip events overlapping at Pallett Creek and separated by only a couple of years or less would be unlikely using the sedimentary record at the site, and so we must acknowledge the remote possibility that any of the earthquake horizons could represent two very closely timed events.

A much more significant issue is the possible occurrence of two large displacements during a several-decades-long or century-long hiatus in deposition at Pallett Creek. To investigate this possibility, we must consider which earthquake horizons sit at such hiatuses. The new, more precise dates provide a much clearer indication of this than did the old dates.

An examination of the calendric dates presented in Table 2 and Figure 1 and consideration of the refinements discussed in the text above reveal that one of the latest 10 events occurred during a hiatus in deposition of more than a decade. Event T, which occurred A.D. 1346 (1329–1363), was followed by about half a century of little or no deposition. Peat deposition recommenced A.D. 1408 (1397–1419) with deposition of lowest unit 68. Therefore it is conceivable that a slip event occurred in the latter half of the fifteenth century that cannot be distinguished from event T. As *Sieh* [1984] pointed out, however, the occurrence of such an event would mean that the measured lateral slip for event T (about 1.3 m) would have to be shared by T and that later event. Thus, if the hypothetical event were the same size as T, T would necessarily be halved in size.

Two events, R and X, were followed by deposition of massive units. Earthquakes occurring during the time of deposition of these massive units might well be obscured in the geologic record. Hence we must consider the possibility of earthquakes between events X and Z and between events R and T.

The former of the two hypothetical earthquakes would have to have occurred between A.D. 1812 and A.D. 1857 if event X is the event discovered by *Jacoby et al.* [1987, 1988] in trees southeast of Pallett Creek. The occurrence of a large slip event at Pallett Creek during this period is very unlikely. Except for the 1812 earthquake, the historical record contains no mention of an earthquake as severely and extensively felt as the 1857 event. One man, who lived in the Los Angeles region throughout most of the 60 years prior to 1857 stated, in fact, that these were the only two severely and extensively felt

earthquakes to occur in the area during the first half of the century [*Agnew and Sieh*, 1978, microfiche item 12].

Another possibility can be entertained if one is willing to reject Jacoby et al.'s arguments that event X is the earthquake of A.D. 1812. If event X occurred earlier in the date range A.D. 1785 (1753–1817), the 1812 earthquake would be the second of three tightly clustered events. An even more remote possibility is that event X occurred A.D. 1688 (1675–1701). In this case, event X would have occurred about two centuries after event V, and the event X/1812/1857 cluster would have occurred over a period of about 170 years. In our judgment, both of these scenarios are unlikely, and event X is probably the earthquake of A.D. 1812. Accepting this, the historical evidence favors the quiescence of the fault between event X and 1857.

An earthquake between events R and T is more problematic. Such an event could have occurred during deposition of massive unit 59. This unit was deposited between A.D. 1100 (1035–1165) (event R) and A.D. 1233 (1215–1250) (deposition of lowest unit 61). The existence of this event is unlikely, because *Sieh* [1978*a*, 1984] found no evidence of liquefaction or faulting associated with a horizon within unit 59. If, however, an earthquake is hidden in the section at Pallett Creek, this is one of the three plausible locations.

Summarizing this section, we do not consider hidden events likely; we have no evidence for any events other than those previously identified by *Sieh* [1978*a*, 1984]. But we acknowledge the possibility that events could be hidden in three intervals: About 1100 to about 1235, about 1346–1400, and between about 1688 and 1812.

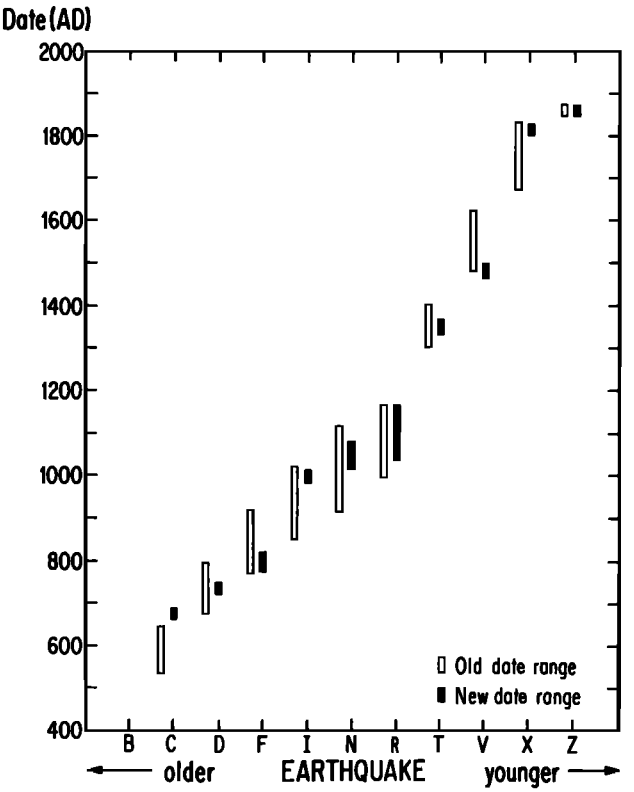

Fig. 7. A comparison of the new earthquake dates and those derived from radiocarbon analyses published earlier shows that all but one of the new date estimates are enclosed within or overlap the broader date estimates of *Sieh* [1984].

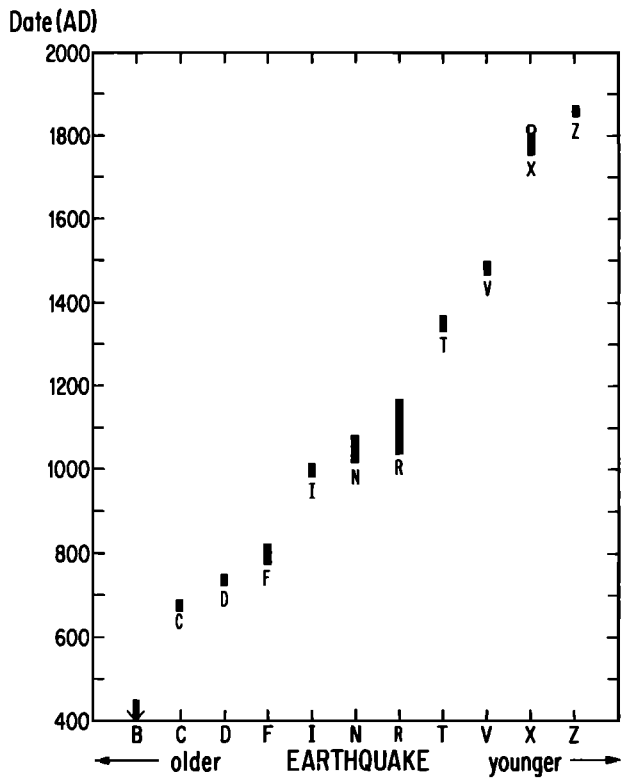

Fig. 6. New estimates of the dates for earthquakes recorded in the sediments at Pallett Creek. Bars give 95% confidence intervals. Open circle on bar of event X indicates preferred date of A.D. 1812.

Average Recurrence Interval

Previously published earthquake dates lead to an estimated average interval between the latest 12 events at Pallett Creek of about 145 years [*Sieh*, 1984]. In this paper we have concluded that the date range for the oldest known event, event A, is too poorly constrained to use in recalculating the average interval. Instead, we calculate an average interval using the oldest precisely dated event, that is, event C, and the most recent event, event Z.

The estimated average period of dormancy between A.D. 671 (event C) and A.D. 1857 (event Z) is 132 years, assuming nine intervals. The 95% confidence interval for the mean recurrence interval is 130.3–133.2 years. The average interval for the latest 10 events estimated using the old date for event C, A.D. 590, was 141 years. Hence the new estimate is about a decade shorter than the previous estimate. Coincidentally, 132 years is equal to the current (1988) period of dormancy.

If two of the 10 events are not large, the estimated average interval for large earthquakes increases to 169 years. This possibility is discussed by *Sieh* [1984]. If two large events are hidden in the section, the estimated average interval decreases to 108 years. These intervals are calculated to illustrate the plausible range in average interval estimates. In fact, it seems most reasonable to take 132 years as the best estimate of the average interval between large slip events at Pallett Creek.

Having estimated an average interval it is now important to discuss the distribution of the individual values about that average. Table 4 lists the individual intervals and their uncer-

TABLE 4. Recurrence Intervals for Earthquakes at Pallett Creek

Events	Interval
X–Z	44 years
V–X	332 (317, 347)*
T–V	134 (111, 157)
R–T	246 (179, 313)
N–R	52 (−21, 125)
I–N	52 (15, 89)
F–I	200 (173, 227)
D–F	63 (37, 89)
C–D	63 (45, 81)

A 95% confidence interval for the mean recurrence interval is 130.3 (1857–684)/9 to 133.2 (1857–658)/9 years.
*95% confidence limits.

tainties. Normally, one would calculate a standard error by

$$[\sum (x - \bar{x})^2/(n - 1)]^{1/2}$$

The two standard error estimate in this case would be 105 years. For two reasons this calculation is not appropriate in the present case. First, the intervals are estimates not known values; second, the estimates are highly correlated. We note these complications here and now proceed to discuss the data further.

Estimates of the Probability of a Large Earthquake in the Near Future

Several attempts have been made in recent years to calculate probabilities associated with large earthquakes along the San Andreas fault [*Sieh*, 1984; *Lindh*, 1983; *Sykes and Nishenko*, 1984; *Wesnousky*, 1986; *Working Group on California Earthquake Probabilities*, 1988]. These calculations have been motivated in large part by the great societal value of earthquake forecasts. Lindh's, Sieh's, and some of Sykes and Nishenko's calculations were based upon the dates of events at Pallett Creek. Lindh's estimate (a 40% likelihood in the next 30 years) was made assuming that each of the recorded events is large, that there are no missing large events, that there are no trends or patterns in the recurrence intervals, and that the recurrence intervals are distributed about the mean interval according to a Gaussian distribution function. Sieh's estimates took into account a wider range of possibilities; for example, he considered both that some of the events might be small and that trends toward shorter and shorter recurrence intervals might exist. He calculated a range of probabilities of a large earthquake of between 26% and 98% for the next 50 years. Sykes and Nishenko estimated a probability of about 10% for the period 1983–2003, assuming a Weibull distribution function for the earthquake dates and assuming a recurrence interval of 194 years (they assumed that two of the events were not large earthquakes).

For the guidance of civil emergency planners and for comparison with these previous estimates, we have estimated the conditional probability of a future large earthquake, using the new dates of the past 10 events. As in two of the papers cited above, the record is assumed to be complete; that is, we assume no events remain undiscovered at the site. In addition, we assume that all of the recorded events are large. Following *Jeffreys'* [1967, pp 1398–1401] stricture that "An estimate without a standard error is practically meaningless," we indicate the uncertainties of our estimates, and these are seen to be large. Our probabilistic estimates have been made using a Weibull distribution, in a manner that is an extension of that employed by *Brillinger* [1982] to estimate probabilities from earlier date estimates. We choose to use the Weibull distribution because it has proven useful in a broad variety of similar applications, particularly lifetime modeling, and because it stands up to an assessment of goodness of fit with the data. It is appropriate in the case of earthquake recurrence because unlike lognormal and some other lifetime distribution functions, the Weibull is characterized by its steadily increasing hazard function for a range of parameter values. It is defined by the cumulative distribution function

$$F(x) = \text{Prob}\{\text{result} < x\} = 1 - \exp\{-(x/\alpha)^\beta\} \qquad x > 0$$

with α and β being unknown parameters. In the present context, "result" refers to the interval between events. The hazard function associated with the Weibull is given by

$$h(x) = (\beta/\alpha)(x/\alpha)^{\beta - 1} \qquad x > 0$$

with the interpretation

$$\text{Prob}\{x < \text{interval} < x + \Delta | \text{interval} > x\} = h(x)\Delta$$

for small Δ. It provides the rate of earthquake occurrence, given that the last event occurred x years previously. For $\beta > 1$, the hazard of the Weibull increases steadily. The shape parameter β has been related to the stress-strain relation of the medium and in particular to whether the medium is elastic [see *Martinez et al.*, 1987]. Its reciprocal is the slope of the ideal line in the hazard plot, discussed below.

The plausibility of the Weibull distribution for a sequence of interevent intervals may be examined by preparing a Weibull hazard plot. Briefly, observed intervals are plotted on a particular graph paper, treating the final open interval specially. Then one checks to see if the points fall near a straight line to assess validity of fit [*Nelson*, 1982]. Figure 8 provides a Weibull hazard plot for the intervals of Table 4 and the current open interval of 131 years. Error bars have been included for the intervals. Examination of the graph suggests that the Weibull assumption is not unreasonable. The straight line graphed is the maximum likelihood estimate of the theoretical relationship. Its derivation is discussed in the appendix. Spe-

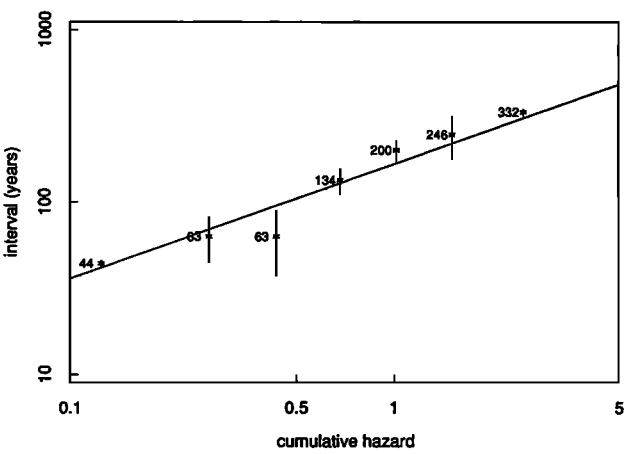

Fig. 8. Cumulative Weibull hazard plot based on the interevent time estimates 44, 63, 63, 134, 200, 246, 332 years and the open interval of 131 years.

cial difficulties that arose in the analysis were the existence of the current open interval and the interpolated date for event N. How they were dealt with is indicated in the appendix.

We have chosen to represent the probabilities we have estimated in two ways. These are illustrated in Figures 9 and 10. Figure 9 displays the cumulative probability of an earthquake for any period of time within the next 100 years, that is, Prob{event within u years from 1988 given last event in 1857}. In terms of $F(x)$, above, this is given by

$$[F(131 + u) - F(131)]/[1 - F(131)]$$

Estimates of this function are based on maximum likelihood estimates of the α and β of the Weibull (see the appendix). The dashed curves provide 95% confidence intervals. By way of example, the estimate of the probability of an earthquake within a year is 0.8% (confidence interval 0.4–2.6%); the estimate of probability within the next 30 years is 22% (confidence interval 7–51%); and the estimate of probability of an earthquake within the next 50 years is 35% (confidence interval 11–71%).

Figure 10 displays the probability of the earthquake for all 30-year periods, beginning between 1988 and 2088, that is, Prob{event within 30 years from year t given last event in 1857}. In terms of $F(x)$, above, this is given by

$$[F(t - 1857 + 30) - F(t - 1857)]/[1 - F(t - 1857)]$$

Estimates of this function are also based on maximum likelihood estimates of the α and β of the Weibull (see the appendix), and the dashed curves provide 95% confidence intervals. For example, for the 30-year period beginning in 1988, the estimated probability is 22% (confidence interval 7–51%).

Regardless of the manner of display, the uncertainty in the probability estimates is large, even though simple geological assumptions have been made. The estimates of α and β were 166.1 ± 44.5 and 1.50 ± 0.80, respectively. *Brillinger* [1982] took the estimate of β to be 2, corresponding to a Rayleigh distribution. The value $\beta = 1$ corresponds to an exponential distribution for the intervals. Because of the large standard error 0.80, the exponential distribution, which corresponds to a Poisson distribution of occurrence times, can not be ruled out for these data.

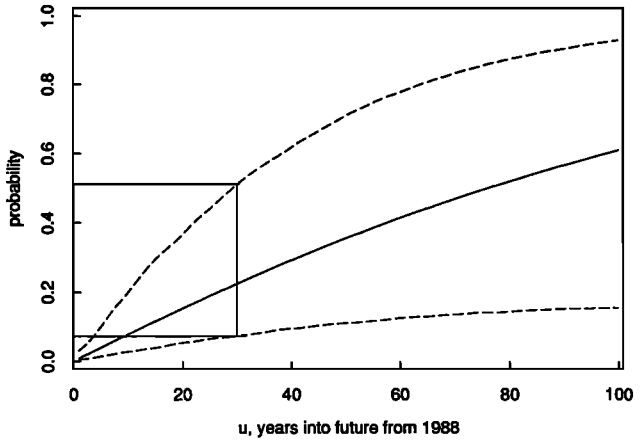

Fig. 9. Probability of a major fault rupture at Pallett Creek, during the next "u" years, based on the fitted Weibull distribution. Probability estimate for the next 30 years (1988–2018) is illustrated. The parameters of the Weibull are estimated by maximizing the likelihood based on the values 44, 63, 63, 134, 200, 246, and 332 for a Weibull, the value 131 for a censored Weibull, and the value 103 for the sum of two Weibulls. The dashed curves give 95% confidence intervals for the estimated probabilities, taking note of the uncertainty of the Weibull fit but not of the date estimates themselves.

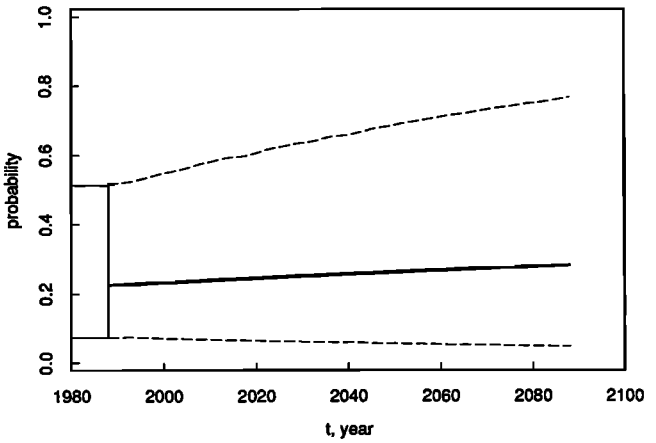

Fig. 10. Probability of a major fault rupture at Pallett Creek, during any 30-year period beginning between 1988 and 2088. Probability estimate for the 30-year period beginning in 1988 is illustrated.

It is curious that even though the new average interval is about 10% shorter than the previously published value, the point estimate of the probability of a large earthquake is less than previous estimates. This is due to the fact that the distribution of apparent intervals about the mean is now much broader than was assumed in previous calculations.

Because of uncertainties in interpretation of the Pallett Creek data the probabilities given above should be viewed as only one plausible approximation of the hazard posed by the segment of the San Andreas fault closest to Los Angeles. Higher probabilities are calculated if one assumes that one or more large earthquakes are hidden in the section. Lower probabilities are derived if one assumes that two of the events are not large earthquakes [*Sieh*, 1984].

Perhaps more significantly, the staircaselike pattern displayed in Figure 6 suggests that the periods of quiescence between large earthquakes may be bimodally distributed. The significance of this pattern is discussed in the following sections.

Marked Variability in the Length of Earthquake Cycles

The principal scientific value of the new, more precise earthquake dates may not be refinement of probabilistic estimates but rather the temporal pattern that they suggest. In fact, the probabilistic estimates derived from the new dates have uncertainties so large that they encompass most estimates by previous workers. For example, the estimate made by the *Working Group on California Earthquake Probabilities* [1988], that the Mojave segment of the San Andreas fault has a 30% probability of generating a major earthquake during the next 30 years, is well within the 7–51% range that we have estimated using the new data.

Although the new dates do not enable a narrowing of probabilistic earthquake forecasts, they do suggest tantalizing possibilities for the mechanical behavior of the fault.

Immediately apparent from Table 4 and Figure 6, which show the intervals between the past 10 earthquakes, is the fact

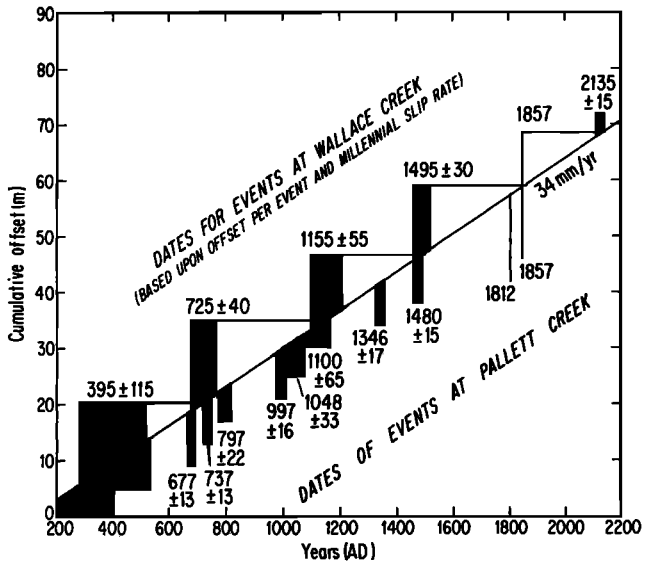

Fig. 11. Comparison of earthquake dates derived from the Pallett Creek site and those estimated from the Wallace Creek site. The date ranges determined from Pallett Creek are shown as vertical bands beneath the diagonal line. The date ranges above the line are derived by dividing the amount of offset during a past earthquake at Wallace Creek by the long-term slip rate there. See text for discussion. In this figure the length of the earthquake cycle is assumed to be proportional to the amount of offset during the earthquake at the beginning of the cycle. The figure suggests that the second or third earthquake in each cluster at Pallett Creek involves rupture at Wallace Creek and that the first event in each cluster does not.

that the interval between slip events at Pallett Creek ranges markedly from the mean of 132 years. Five of the latest nine intervals are less than 100 years. Three intervals are between about 200 and 330 years.

Furthermore, the latest 10 events appear to cluster in four groups. Within the clusters, intervals between earthquakes are mostly less than 100 years. The time between clusters, however, is between about 200 and 330 years. The new dates are precise enough that the occurrence of this clustering cannot be easily disputed.

The effect of inserting missing events into the record would probably only accentuate the clustering because two of the three periods that are candidates for harboring missing events occur within, not in between, clusters. These are the periods between events T and V and between events X and Z. Of the three long intervals between clusters, only one (between events R and T) could conceivably be split into two shorter intervals by an undiscovered event. Even if one embraces the less likely date range of 1688 (1675–1701) for event X and assumes a hidden earthquake between events R and T, intervals would range between about 50 and 200 years.

Temporal clustering of large earthquakes has been observed in other regions, and so its recognition here might not be all that surprising. *Lee and Brillinger* [1979] suggest that the historical record of central China documents four century-long clusters of large earthquakes since about A.D. 1000. In this century, bursts of large earthquake sequences have occurred in the Aleutians (1957–1965), in Turkey (1939–1944), and elsewhere. The Pallett Creek data may, however, be the first indication of temporal clustering of large earthquakes along one segment of a fault.

An interesting and important question arises if one assumes that the clustering displayed in Figure 6 will continue for the next few earthquake cycles: Will the present interval complete a cluster or will it separate the end of the last cluster from the beginning of the next? That is, will the present open interval be long, or will it be short?

A qualitative response to this question can be formulated simply by examination of Figure 6. Five of the six intracluster intervals span less than a century; the other intracluster interval (T–V) was about 134 years long. This suggests that the present open interval of 131 years is probably not an intracluster interval. Rather, it is more likely to be a long interval separating clusters. If it is going to be an interval separating the latest cluster from the next, the probability of earthquake occurrence within the next 30 years is quite low, less, in fact, than the 22% probability calculated above.

The existence of a mechanical reason for the clustering is an intriguing possibility. *Rundle* [1988] has argued, on the basis of his theoretical modeling of the San Andreas fault, that clustering of large earthquakes is an expectable consequence of the strong interaction of neighboring fault segments. We wonder if the temporal clustering in the data from Pallett Creek represents clustering of great earthquakes along the southern portion of the fault. To explore this possibility, we have, in the following section, used paleoseismic data from other sites along the fault in conjunction with our data to constrain the geographical limits of paleoearthquakes.

Possible Correlations of Pallett Creek Events With Those at Other Sites

The precision of the new Pallett Creek dates encourages us to attempt correlations with earthquakes recorded at other paleoseismic sites along the southern half of the San Andreas fault. If we could accurately correlate events at Pallett Creek with those identified at other sites along the San Andreas fault, we would be able to establish more firmly the lengths and locations of individual fault ruptures. Data of this sort would provide important clues about the mechanical behavior of the fault.

Figures 13 and 14 summarize our attempts to resolve the spatial and temporal history of large earthquakes. The speculations embodied by these figures are based upon the information and interpretations presented in the following.

First, we consider plausible correlations of Pallett Creek events with events recorded by offset gullies in the Carrizo Plain, about 200 km northwest of the Pallett Creek site. In the Carrizo Plain, near a large offset drainage called Wallace Creek, *Sieh* [1978*b*] and *Sieh and Jahns* [1984] documented gullies offset about $9\frac{1}{2}$ m during the 1857 earthquake. They also measured larger offset values. These they interpreted as evidence for several large earthquakes, each associated with dextral slip of between 11 and 15 m.

One can calculate hypothetical dates for these prehistoric earthquakes by dividing the long-term slip rate (34 ± 3 mm/yr) determined at Wallace Creek into the offsets recorded for the several earthquakes. Such calculations assume, of course, that the amount of strain accumulated between large slip events is related to the amount of slip that occurs during the earthquake that occurs either at the end or at the beginning of the cycle.

Figures 11 and 12 display the results of two sets of calculations made in this way. In both cases the long-term slip rate is represented by the sloping line. The line passes through the

point (A.D. 1857, 59 m). Fifty-nine meters is the largest gully offset measured by *Sieh and Jahns* [1984, Figure 8].

In Figure 11 we have assumed that the length of an earthquake cycle is related to the slip experienced during the large earthquake that preceded it. For example, the interval between 1857 and the next large earthquake is estimated by dividing the $9\frac{1}{2}$-m offset of 1857 by the long-term slip rate. This interval is added to A.D. 1857 to estimate the date of the next large earthquake: A.D. 2135 (2120–2150). To estimate the date of the earthquake that preceded the 1857 event, the offset associated with that last prehistoric earthquake, 12.3 ± 1.2 m, is divided by the long-term slip rate, and the quotient is subtracted from A.D. 1857. The date thus estimated is A.D. 1495 (1465–1525). Similarly, dates of A.D. 1155 (1100–1210), 725 (685–765), and 395 (280–510) are estimated for the previous three large events.

In Figure 12 we have assumed that the length of the earthquake cycle is related to the amount of slip experienced during the large earthquake that occurred at the end of that cycle, rather than at the beginning. Dates for the last four prehistoric events are estimated to be A.D. 1580 (1565–1595), 1220 (1190–1250), 875 (820–930), and 445 (400–490).

In both Figures 11 and 12 the dates of the earthquakes at Pallett Creek are shown as vertical bars for comparison with the estimated dates. In Figure 12 the events at Wallace Creek occur during the long periods between clusters at Pallett Creek. In Figure 11, however, the events at Wallace Creek seem to correlate with the last or middle event in each cluster. The last prehistoric event at Wallace Creek (in A.D. 1495 (1465–1525)) occurred within the date range of event V (A.D. 1480 (1465–1495)). The previous event is within the date range of event R, and the previous two events are within the date ranges of events D and B.

The possibility that slip events at Wallace Creek correlate with the last or middle event in each cluster at Pallett Creek is intriguing. Perhaps the last large event in each cluster is an event like the great 1857 event, that is, an event that involves rupture of the Cholame, Carrizo and Mojave segments of the fault (see Figure 13 for location of these segments). And perhaps the earlier one or two large events in each cluster represent events which involved rupture of the Mojave segment alone or the Mojave segment in concert with the San Bernardino and Indio segments to the southeast. Such alternation of large ruptures has been proposed by *Sieh* [1978*a*], *Weldon and Sieh* [1985], and *Sykes and Seeber* [1985].

The new dates at Pallett Creek are precise enough to enable a weak test of this hypothesis. Using data from all of the paleoseismic sites along the southern half of the fault, which are labeled in Figure 13, we will attempt to correlate dated events. The uncertainties in radiocarbon dating of earthquakes at each site precludes us from being certain of any of the correlations, of course.

In Figures 13 and 14, we give those ruptures documented and dated at Pallett Creek the greatest lengths allowed by the data from the other sites. This seems to be the most reasonable assumption, given that both the great 1906 and 1857 earthquakes were generated by fault ruptures that spanned several hundred kilometers of the fault.

Figure 13 displays six proposed large earthquake ruptures. The oldest event, R, is in the lower right box, and the youngest event, Z, is in the upper left box. The following paragraphs justify this version of history.

Event Z. Event Z is known to be the earthquake of A.D. 1857. Historical accounts indicate that the fault ruptured the Cholame, Carrizo, and Mojave segments of the fault [*Sieh*, 1978*b*] and not the San Bernardino segment [*Agnew and Sieh*, 1978].

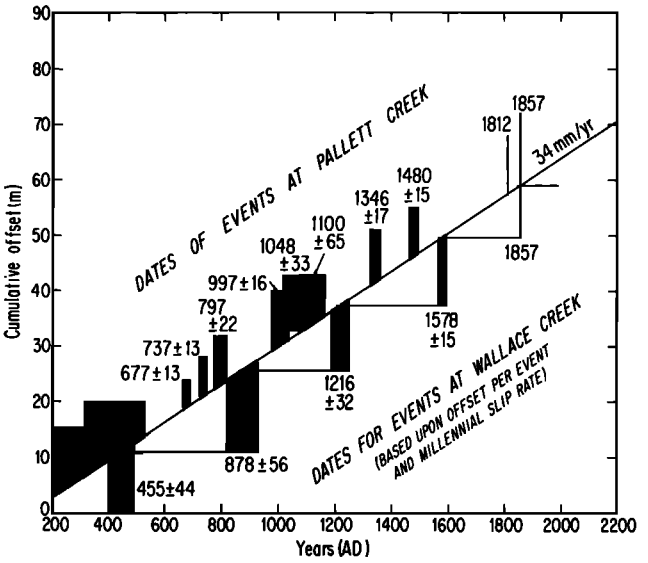

Fig. 12. Same as Figure 11 except that the length of the earthquake cycle is assumed to be proportional to the amount of offset during the earthquake at the end of the cycle. This figure suggests that Wallace Creek events occurred during periods of repose at Pallett Creek.

Event X. Event X is probably the earthquake of December 8, 1812. *Jacoby et al.* [1988] propose the rupture length indicated in Figure 13 as the most reasonable. Consideration of Figures 11 and 12 leads us to the conclusion that no slip events occurred near Wallace Creek, along the Carrizo segment, in the 300 years prior to 1857. An event has been dated at Mill Potrero, however, at A.D. 1670–1775 or 1793–1948 (event II of *Davis* [1983]). These date ranges were recalculated by us from Davis's data from Mill Potrero, using the new calibration curves. These calculations assume a lab error multiplier of 1.6, the $\delta^{13}C$ values assumed, but not measured, by the laboratory that analyzed the samples, and a confidence limit of 95%.

Evidence from the Indio and Ferrum sites suggests that no large event has involved rupture of the Indio segment since about A.D. 1680 [*Sieh*, 1986; *Williams and Sieh*, 1987; K. Sieh and P. L. Williams, manuscript in preparation, 1988]. As much as a half meter of slip at these sites may be associated with an earthquake after about 1680, but such a small offset would probably be associated with an earthquake of $M < 7$ or with aseismic slip. On the basis of this fragmentary evidence, we speculate in Figure 13 that event X involved only rupture of the Mojave segment, part of the San Bernardino segment and the southeastern portion of the Carrizo segment.

Event W. This event is recorded at the Indio site and is associated with at least 2 m of dextral slip there [*Sieh*, 1986]. The record at Pallett Creek clearly shows that no slip event affected the site between event V and event X. Radiocarbon and dendrochronologic analyses indicate that the dates of these events are A.D. 1480 (1465–1495) and A.D. 1812. Event W, then, probably involved rupture of only the Indio segment and, perhaps, the San Bernardino segment. The remote possi-

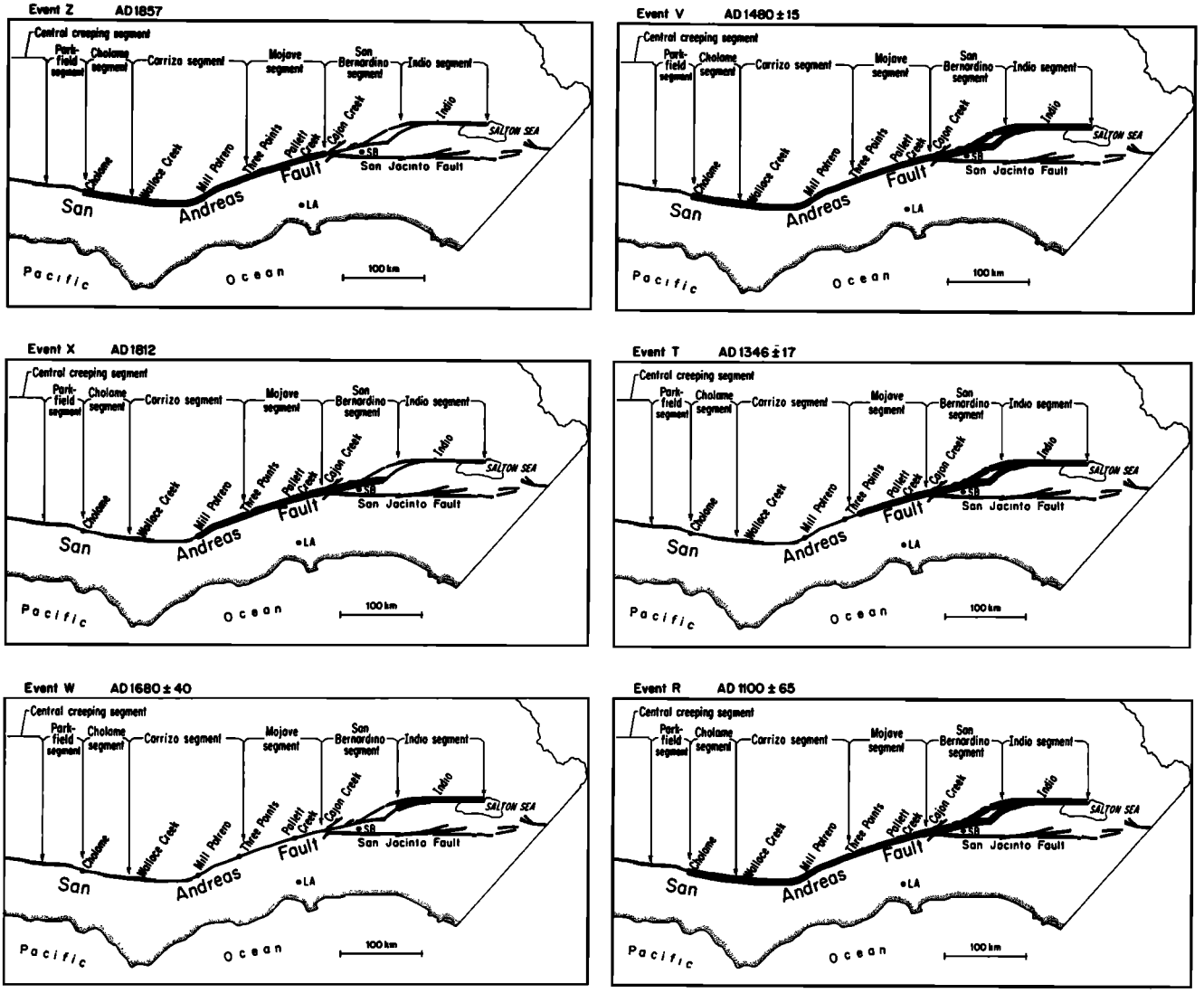

Fig. 13. Plausible earthquake history for the southern half of the San Andreas fault for the past millennium. See text for discussion of data and assumptions.

bility that event X occurred during the period A.D. 1688 (1675–1701) is adopted in constructing the alternative historical scenario represented by Figure 14.

Event V. This event could conceivably have ruptured the entire southern half of the San Andreas fault. Figure 11 suggests that the last prehistoric rupture in the Carrizo Plain, which involved about 12.3 m of dextral slip, is event V. At Mill Potrero a large slip event occurred within the range A.D. 1435–1672 (Davis's event I, date recalculated by us). At the Indio site an event involving at least 3.5 m of dextral slip occurred A.D. 1450 (1300–1600). In Figure 13 we assume that this event is the same as event V at Pallett Creek. An alternative possibility, that it correlates with event T, is used in the construction of Figure 14.

Event T. Figures 11 and 12 suggest that no events near Wallace Creek correlate with event T. Correlation of event T with an event at the Indio site dated at A.D. 1300 (1210–1390) is plausible. We assume this correlation and show on Figure 13 the Mojave, San Bernardino, and Indio segments breaking during event T.

Event R. Like event V, this event may have involved rupture of the entire southern half of the San Andreas fault. Figure 11 suggests that this event, or event N, may have been an event that resulted in about 11 m of slip near Wallace Creek. Data from the Indio and Salt Creek sites permit a large event during this period as well.

The correlation of events proposed above and illustrated in Figure 13 is speculative and is intended only to provoke discussion and further paleoseismic studies and theoretical modeling. If the historical scenario of Figure 13 is roughly correct, the past three large earthquakes along the southern half of the fault progressed from southeast to northwest during a period of about 170 years. Two of the three previous large events in this case ruptured the entire southern half of the fault.

Figure 14 illustrates a less likely, but plausible alternative historical scenario. In this case, we assume event X occurred A.D. 1688 (1675–1701) and that evidence of the 1812 earthquake at Pallett Creek is hidden in the massive unit between events X and Z. We also correlate the A.D. 1450 (1300–1600) event at Indio with event T at Pallett Creek. This scenario presents a more regular pattern of earthquake occurrence; in it three northwestward progressions of large earthquakes occur: one between A.D. 1000 and 1100, another between A.D. 1300 and 1480, and another between A.D. 1680 and

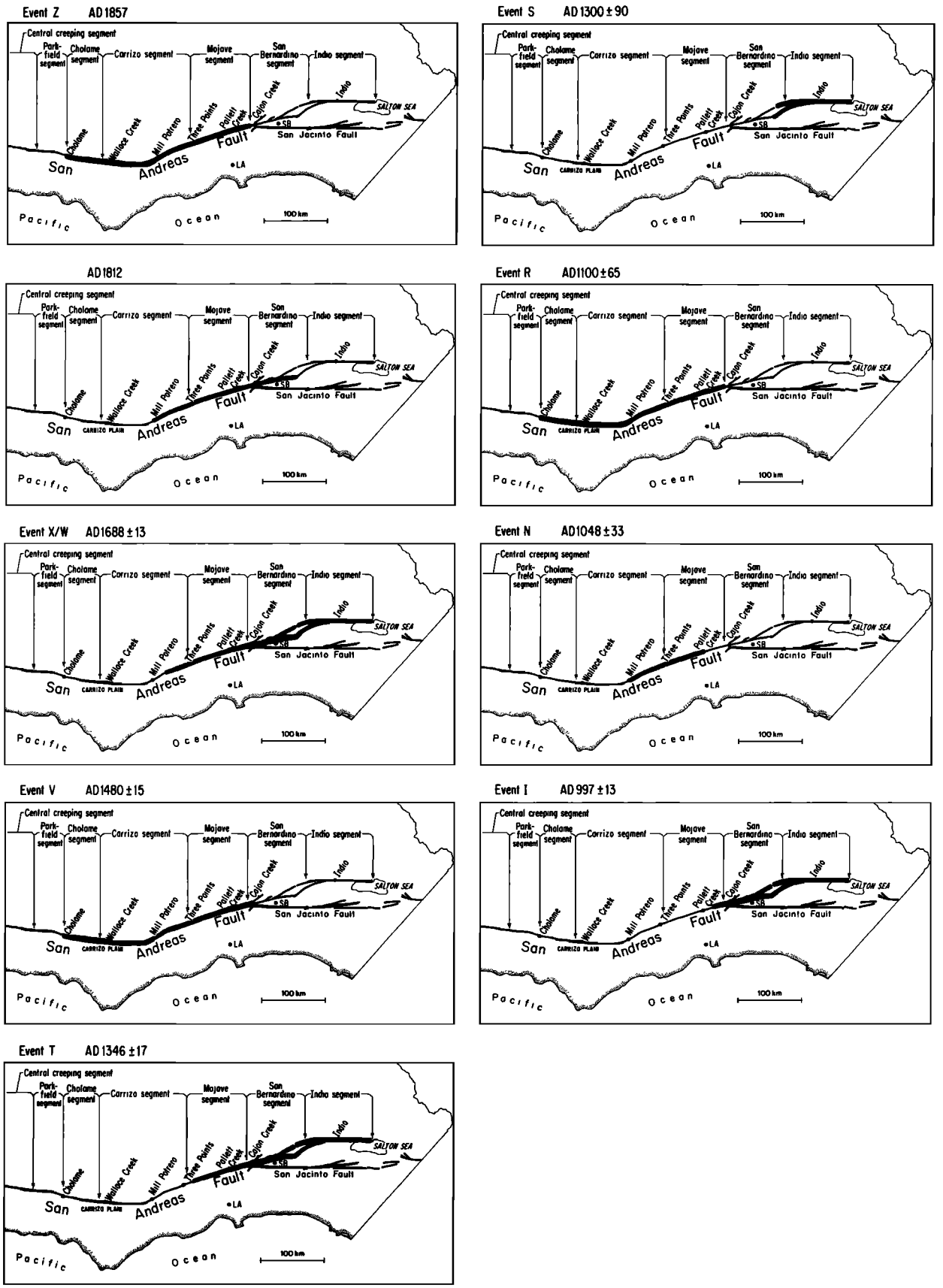

Fig. 14. Less likely but plausible alternate earthquake history for the southern half of the San Andreas fault. This scenario contains three northwestward progressions of large earthquakes that correlate with the temporal clusterings of earthquakes at Pallett Creek that are shown in Figure 6.

1857. Each of these progressions involves overlapping ruptures along the Mojave segment of the fault and corresponds to one of the periods of earthquake clustering in the record at Pallett Creek.

Other viable earthquake scenarios, consistent with the sparse data now available, can be constructed. If, for example, one abandons the attempt to make the earthquake ruptures as large as the paleoseismic data allow, the possibilities are legion. We believe that more precise dating of slip events at paleoseismic sites other than Pallett Creek will lead to more certain correlation of earthquake ruptures between sites. This would enable more reliable estimates of magnitude for prehistoric events and recognition of spatial and temporal patterns of large earthquake occurrence.

CONCLUSIONS

A better understanding of the geological processes of which large earthquakes are the most notorious part will likely improve as the history of past events becomes better known. The data presented in this paper are a step in that direction. We show that the dates of prehistoric earthquakes along the San Andreas fault can be determined with errors of only a couple of decades. More precise dating and characterization of large prehistoric earthquakes elsewhere along the fault may enable correlation of events between paleoseismic sites. This might reveal temporal and spatial patterns of large earthquakes that have resulted from interacting faults or fault segments, or from nonuniform regional strain accumulation or strain relief. A better understanding of the causes of such behavior is of great significance to society because it might well lead to reliable long-term and short-term forecasts of fault behavior.

APPENDIX

The estimation of an unknown quantity (or parameter) is often conveniently approached via the likelihood function. This is a specific function of an assumed stochastic model and data meant to provide a measure of the weight of evidence for the various possible values of the parameters. It may be used to construct point estimates or confidence intervals in particular or to combine distinct measurements.

For the dated samples of this paper the likelihood may be set down as follows: Let u denote radiocarbon age. Let t denote calendric date. Let

$$u = \hat{g}(t)$$

denote the estimated calibration curve with estimated standard error $\hat{s}(t)$ at t (these are given by *Stuiver and Becker* [1986]). Let U denote a sample's estimated radiocarbon age and S its estimated standard error. Then, assuming that the errors are approximately normal, the likelihood function is given by

$$[s^2 + \hat{s}(t)^2]^{-1/2} \exp\{-\tfrac{1}{2}[U - \hat{g}(t)]^2/[S^2 + \hat{s}(t)^2]\} \quad \text{(A1)}$$

scaled to have value 1 at the minimum. This may be approximated by dropping the first factor. This expression may be plotted as a function of t to see the relative evidence for the various values of t. An approximate 95% confidence interval for the value of t is provided by the collection of t values such that (A1) exceeds 0.1465. Figure 3 provides a variety of examples. Sometimes, because the calibration curve is not single-valued, the confidence interval breaks into two intervals.

The likelihood function may also be used to estimate unknown parameters. Given observations $x_1, x_2, \cdots$ from independent distributions depending on an unknown parameter θ, the likelihood is given by

$$f_1(x_1, \theta) f_2(x_2, \theta) \cdots f_n(x_n, \theta)$$

with $f_1(x, \theta)$ representing the density of x_1. The parameter θ may be estimated by maximizing this likelihood, and expressions are available for standard errors [*Nelson*, 1982]. In the present situation, seven of the x refer to intervals of the Weibull, one refers to the present open (censored) interval of 131 years and one, surrounding event N, to the sum of two Weibulls. The term for the censored value is simply $1 - F(131)$. The term for event N is derived by numerical integration. The uncertainties of the interval lengths have been ignored in the maximum likelihood computations presented.

Acknowledgments. This study was supported by the U.S. Geological Survey (USGS) as part of the National Earthquake Hazards Reduction Program. Support for Sieh was through USGS grant 14-08-0001-G1086 and contract 22026. Brillinger was supported through U.S. Geological Survey grant 14-08-0001-G1085 and NSF grant DMS-8316634. Stuiver was funded through U.S. Geological Survey grant 14-08-0001-G1083. Norman Brown and Paul Haase assisted in collection and processing of some of the samples, and Janice Mayne and Stephen Salyards assisted in preparation of some of the figures. We appreciate the critical reviews of James Lienkaemper, Stuart Nishenko, Carol Prentice, and Ross Stein and discussions with David Schwartz and many others. This paper is Caltech, Division of Geological and Planetary Sciences contribution 4583.

REFERENCES

Agnew, D., and K. Sieh, A documentary study of the felt effects of the great California earthquake of 1857, *Bull. Seismol. Soc. Am.*, *68*, 1717–1729, 1978.

Brillinger, D., Seismic risk assessment: Some statistical aspects, *Earthquake Predict. Res.*, *1*, 183–195, 1982.

Davis, T., Late Cenozoic structure and tectonic history of the western "Big Bend" of the San Andreas fault and adjacent San Emigdio Mountains, Ph.D. dissertation, 580 pp., Univ. of Calif., Santa Barbara, 1983.

Jacoby, G. C., P. R. Sheppard, and K. E. Sieh, Was the 8 December 1812 California earthquake produced by the San Andreas fault? Evidence from trees near Wrightwood, *Seismol. Res. Lett.*, *58*(1), 14, 1987.

Jacoby, G., P. Sheppard, and K. Sieh, Irregular recurrence of large earthquakes along the San Andreas fault—Evidence from trees, *Science*, *241*, 196–199, 1988.

Jeffreys, H., Statistical methods in seismology, in *International Dictionary of Geophysics*, pp. 1398–1401, Pergamon, New York, 1967.

Lee, W., and D. Brillinger, On Chinese earthquake history—An attempt to model an incomplete data set by point process analysis, *Pure Appl. Geophys.*, *117*, 1229–1257, 1979.

Lindh, A., Preliminary assessment of long-term probabilities for large earthquakes along selected segments of the San Andreas fault system in California, *U.S. Geol. Surv. Open File Rep.*, *83-63*, 1–5, 1983.

Martinez, S., J. San Martin, E. Scheihing, and V. H. Salinas, Theoretical advances on the interoccurrence time distribution of great earthquakes and statistical fitness on Chilean data, report, Dep. of Math. and Comput. Sci., Univ. of Chile, Santiago, 1987.

National Academy of Sciences, *Active Tectonics*, 266 pp., National Academy Press, Washington, D. C., 1986.

Nelson, W., *Applied Life Data Analysis*, John Wiley, New York, 1982.

Rundle, J., A physical model for earthquakes, 2, Application to southern California, *J. Geophys. Res.*, *93*, 6255–6274, 1988.

Rust, D., Trenching studies of the San Andreas fault bordering western Antelope Valley, southern California, in *Summaries of Technical Reports*, vol. XVI, pp. 70–71, National Earthquake Hazard Reduction Program, U.S. Geological Survey, Reston, Va., 1983.

Salyards, S. L., K. E. Sieh, and J. L. Kirschvink, Paleomagnetic measurement of dextral warping during the past three large earthquakes at Pallett Creek, southern California, *Geol. Soc. Am. Abstr. Programs*, *19*(7), 828, 1987.

Sieh, K., Prehistoric large earthquakes produced by slip on the San Andreas fault at Pallett Creek, California, *J. Geophys. Res.*, *83*, 3907–3939, 1978*a*.

Sieh, K., Slip along the San Andreas fault associated with the great 1857 earthquake, *Bull. Seismol. Soc. Am.*, *68*, 1421–1428, 1978*b*.

Sieh, K., Lateral offsets and revised dates of large earthquakes at Pallett Creek, California, *J. Geophys. Res.*, *89*, 7641–7670, 1984.

Sieh, K., Slip rate across the San Andreas fault and prehistoric earthquakes at Indio, California, *Eos Trans. AGU*, *67*, 1200, 1986.

Sieh, K., and R. H. Jahns, Holocene activity of the San Andreas fault at Wallace Creek, California, *Geol. Soc. Am. Bull.*, *95*, 883–896, 1984.

Stuiver, M., A high precision calibration of the AD radiocarbon timescale, *Radiocarbon*, *24*, 1–26, 1982.

Stuiver, M., and B. Becker, High precision decadal calibration of the radiocarbon timescale, AD 1950–2500 BC, *Radiocarbon*, *28*(2B), 863–910, 1986.

Stuiver, M., and R. Kra (Ed.), Calibration issue: Proceedings of the 12th International Radiocarbon Conference, Trondheim, Norway, *Radiocarbon*, *28*(2B), 225 pp., 1986.

Stuiver, M., and P. Reimer, A computer program for radiocarbon age calibration, *Radiocarbon*, *28*(2B), 1022–1030, 1986.

Stuiver, M., S. W. Robinson, and I. C. Yang, ^{14}C dating to 60,000 years B.P. with proportional counters, in *Radiocarbon Dating, Proceedings of the Ninth International Conference, Los Angeles and La Jolla, 1976*, edited by R. Berger and H. E. Suess, pp. 202–215, University of California Press, Berkeley, 1979.

Sykes, L., and S. Nishenko, Probabilities of occurrence of large plate rupturing earthquakes for the San Andreas, San Jacinto, and Imperial faults, California, 1983–2003, *J. Geophys. Res.*, *89*, 5905–5927, 1984.

Sykes, L., and L. Seeber, Great earthquakes and great asperities, San Andreas fault, southern California, *Geology*, *13*, 835–838, 1985.

Weldon, R., and K. Sieh, Holocene rate of slip and tentative recurrence interval for large earthquakes on the San Andreas fault, Cajon Pass, southern California, *Geol. Soc. Am. Bull.*, *96*, 793–812, 1985.

Wesnousky, S., Earthquakes, Quaternary faults, and seismic hazard in California, *J. Geophys. Res.*, *91*, 12,587–12,631, 1986.

Williams, P. L., and K. E. Sieh, Decreasing activity of the southernmost San Andreas fault during the past millennium, *Geol. Soc. Am. Abstr. Programs*, *19*(7), 891, 1987.

Working Group on California Earthquake Probabilities, Probabilities of large earthquakes occurring in California on the San Andreas fault, *U.S. Geol. Surv. Open File Rep.*, *88-398*, 1988.

D. Brillinger, Department of Statistics, University of California, Berkeley, CA 94720.

K. Sieh, Division of Geological and Planetary Sciences, 170-25, California Institute of Technology, Pasadena, CA 91125.

M. Stuiver, Department of Geological Sciences, AK-60, University of Washington, Seattle, WA 98195.

(Received February 23, 1988;
revised July 27, 1988;
accepted July 27, 1988.)